

Novel Cationic Lipids Incorporating an Acid-Sensitive Acylhydrazone Linker: Synthesis and Transfection Properties

Abderrahim Aissaoui,^{†,‡} Benjamin Martin,^{‡,§} Erwan Kan,[§] Noufissa Oudrhiri,[†] Michelle Hauchecorne,[†] Jean-Pierre Vigneron,[§] Jean-Marie Lehn,[§] and Pierre Lehn^{*,†}

INSERM U458, Hôpital Robert Debré, AP-HP, 48 Boulevard Sérurier, 75019 Paris, France, and Laboratoire de Chimie des Interactions Moléculaires, CNRS UPR 285, Collège de France, 11 Place Marcelin Berthelot, 75005 Paris, France

Received March 23, 2004

Cationic lipid-mediated gene transfection involves uptake of the lipid/DNA complexes via endocytosis, a cellular pathway characterized by a significant drop in pH. Thus, in the present study, we aimed to explore the impact on transfection efficiency of the inclusion of an acid-sensitive acylhydrazone function in the cationic lipid structure. We synthesized and evaluated the transfection properties of a series of four cationic steroid derivatives characterized by an acylhydrazone linkage connecting a guanidinium-based headgroup to a saturated cholestanone or an unsaturated cholest-4-enone hydrophobic domain. Acid-catalyzed hydrolysis was confirmed for all lipids, its rate being highest for those with a cholestanone moiety. The compound bis-guanidinium bis(2-aminoethyl)amine hydrazone (BGBH)-cholest-4-enone was found to mediate efficient gene transfection into various mammalian cell lines *in vitro* and into the mouse airways *in vivo*. *In vitro* transfection studies with BGBH-cholest-4-enone formulations also showed that incorporation of a degradable acylhydrazone bond led to low cytotoxicity and impacted the intracellular trafficking of the lipoplexes. Thus, our work allowed us to identify a cationic lipid structure with an acid-cleavable acylhydrazone linker capable of mediating efficient gene transfection *in vitro* and *in vivo* and it thereby provides a basis for further development of related acid-sensitive gene delivery systems.

Introduction

A great number of gene delivery systems, including viral and nonviral vectors, have been developed over the past decade. Recombinant viruses are found to be highly efficient at DNA delivery, but their clinical use is hampered by concerns over antigenicity and cytotoxicity. Nonviral methods are considered safer and show clinical potential but remain less efficient in terms of DNA delivery. Among the various nonviral vectors, cationic lipids are especially attractive because they can be easily prepared and characterized, and each of the constituent parts (headgroup, linker, and hydrophobic anchor) can be modified, facilitating the elucidation of structure–activity relationships.^{1–3} Electrostatic interactions between the positively charged chemical vector and the negatively charged phosphate groups of DNA lead to the spontaneous formation of self-assembled nanometric lipid/DNA complexes, termed lipoplexes. The DNA entrapped in these complexes is protected from nuclease degradation in the extracellular medium and can be delivered to the target cells.

Over the past several years, we have developed a novel class of cationic lipids derived from cholesterol and characterized by a polar headgroup bearing guanidinium functions.⁴ The rationale underlying our approach was that such lipids should combine the membrane-compatible features of the cholesterol subunit and the favorable features of the guanidinium group for

DNA binding. These previous studies have shown that guanidinium cholesterol lipids, in particular bis-guanidinium-tren-cholesterol (BGTC; tren = tris(2-aminoethyl)amine), were efficient and versatile reagents for gene transfection both *in vitro* and into the mouse airways *in vivo*.^{5,6} BGTC liposomes have also been found to be efficient in experimental cancer gene therapy studies involving the delivery of suicide genes in a mouse model of pancreatic peritoneal carcinomatosis⁷ or of the tissue inhibitors of metalloproteinases TIMP-2 and TIMP-3 for hepatocellular carcinoma.⁸

It is generally agreed that lipoplexes enter cells by a nonspecific endocytosis mechanism involving electrostatic interactions between residual positive charges on the complexes and negatively charged cell membrane residues.^{9,10} Endocytosis would deliver the lipoplex to an early endosomal compartment from which the contents must escape if DNA is to avoid degradation by nucleases in the subsequent late endosomes and lysosomes. Several mechanisms have been postulated for endosomal escape of lipoplexes. In particular, Szoka et al. have proposed a model for local endosomal membrane destabilization whereby flip-flop of the anionic lipids from the cytoplasm-facing monolayer of the endosomal membrane is induced by electrostatic interactions with the cationic lipids of the lipoplexes. A neutral ion pair would result leading to endosomal membrane destabilization and dissociation of the DNA from the lipoplex, facilitating its release into the cytosol.^{11,12} Following endosomal escape, the released DNA is then required to traffic to the nucleus in order to permit expression of the transgene. It should be noted, however, that the processes of endosomal escape and

* To whom correspondence should be addressed. Phone: +33(0)-140031932. Fax: +33(0)140031903. E-mail: lehn@idf.inserm.fr.

[‡] Both authors contributed equally.

[†] Hôpital Robert Debré.

[§] Laboratoire de Chimie des Interactions Moléculaires.

nuclear uptake are still not fully understood and remain critical cellular barriers to gene transfection by cationic lipids.^{13,14}

We and others have focused attention onto the nature of the chemical bond linking the hydrophobic and hydrophilic moieties that can play a crucial role in gene delivery by cationic lipids.¹⁵ Indeed, cellular uptake via the endocytosis pathway is characterized by a progressive and significant acidification from the physiological pH (7.4) of the extracellular medium to pH 6.5–6.0 in the endosome and finally to approximately pH 5.0 in the primary and secondary lysosomes.¹⁶ Consequently, we sought a chemical bond that would be sensitive to this specific pH gradient, triggering hydrolysis of the vector and subsequent DNA release. Indeed, if vector hydrolysis in the endosomal compartment were concomitant with endosomal membrane destabilization, dismantling of the lipoplexes and release of DNA into the cytosol would be enhanced and consequently transfection efficiency might be improved. Positive transfection results have already been reported when using lipids with acid-sensitive functions such as vinyl ethers¹⁷ and ortho esters.¹⁸

In the present work, we chose to synthesize and explore the transfection properties of cationic lipids incorporating an acid-sensitive acylhydrazone bond in their linker. Indeed, the use of acylhydrazones for gene delivery is yet to be reported, although acylhydrazones have seen particular success in drug delivery applications.^{19–23} Thus, we herein report the synthesis and characterization of a series of four cationic steroid derivatives incorporating an acid-cleavable acylhydrazone linkage connecting a guanidinium-based headgroup to either a saturated cholestanone or an unsaturated cholest-4-enone hydrophobic moiety. We also report the results of *in vitro* transfection studies that allowed us to identify the compound bis-guanidinium bis(2-aminoethyl)amine hydrazone (BGBH)-cholest-4-enone as the most efficient for gene transfer. Further, BGBH-cholest-4-enone/DOPE liposomes were found to mediate gene transfection into the mouse airways *in vivo*.

Results and Discussion

The development of numerous pH-sensitive conjugates for drug delivery has followed from the recognition that these reagents, once internalized into endosomes, encounter an increasingly acidic environment that can be used for triggering cargo release. Numerous research groups have contributed to the “triggered” approach to drug delivery by preparation and characterization of either acid-sensitive carrier–drug conjugates²³ or drug-encapsulating liposomes.^{15,24} Liposome-mediated delivery can rely on a pH-induced event leading to destabilization of the liposome structure^{25,26} or on cleavage of components crucial for liposome integrity.²⁷ With respect to gene delivery by cationic lipids, the former approach has been explored by use of protonation of imidazole containing amphiphiles^{28,29} and of suitably designed gemini surfactants,³⁰ whereas the latter approach has been illustrated via cleavage of acid-sensitive vinyl ether¹⁷ or ortho ester¹⁸ lipids. Our aim here was to build on our previous experience with the cationic lipid BGTC (where a headgroup bearing two guanidinium functions is linked via a carbamoyl bond to a

hydrophobic moiety consisting of a cholesterol molecule) by preparing novel guanidinium-based vectors that were acid-sensitive. Because acid-labile acylhydrazones functional groups have seen wide ranging usage in drug delivery applications,^{19,21–23} we chose this cleavable group to connect a steroid anchor to a bis-guanidinium polar headgroup. The present report describes the synthesis, characterization, and transfection properties of such novel 3-keto steroid-derived amphiphilic cationic lipids containing a cleavable acylhydrazone bond in their spacer.

Synthesis and Characterization of Acylhydrazone Vectors. Synthesis of the BGBH (bis-guanidinium bis(2-aminoethyl)amine hydrazone) polar headgroup was achieved in four steps starting from diethylenetriamine (Figure 1). Guanidinium groups in their Boc-protected form were added to the primary amino groups using the reagent *N,N*-bis(*tert*-butoxycarbonyl)-1*H*-pyrazole-1-carboxamide to give compound **1** in satisfactory yield. This product could not be stored for an extended period of time because of the formation of a cycloguanidine product, thought to form via nucleophilic attack of the imino bond of the protected guanidine group by the central secondary amino group.³¹ However, immediate alkylation of the central secondary amino group with methyl chloroacetate, and upon isolation, substitution of the methoxy group by hydrazine, gave the acylhydrazone **3** without complications. In the final step the bis-guanidinium acylhydrazone BGBH was obtained by Boc-deprotection using trifluoroacetic acid. The bis-guanidinium acylhydrazone BGTH (bis-guanidinium tris(2-aminoethyl)amine hydrazone) was prepared by a similar synthesis starting from tris(2-aminoethyl)amine onto which was added two Boc-protected guanidine groups. The cationic steroid hydrazones were prepared via an acetic acid catalyzed reaction between BGBH or BGTH and either 5 α -cholestan-3-one or 4-cholesten-3-one to give respectively BGBH-cholestanone, BGBH-cholest-4-enone, BGTH-cholestanone, and BGTH-cholest-4-enone in quantitative yield (Figures 2 and 3). Final compounds were characterized by ¹H and ¹³C NMR, UV spectroscopy, and mass spectrometry including high-resolution FAB (fast atomic bombardment) to confirm the identity of the molecular ions. The ¹H NMR spectra of BGBH-cholest-4-enone and BGTH-cholest-4-enone were particularly informative because of the vinylic 4-H proton, which could be clearly identified downfield of other signals. This signal was indicative of the desired conjugated product due to its coupling to the hydrazone linkage at C-3. *E/Z* isomerism about the keto–hydrazone bond³² could be observed through signal doubling of the vinylic peak, which was further multiplied by restricted rotation around the amido C–N bond,³³ resulting in a total of four vinylic singlets (data not shown). Variable-temperature NMR was employed in order to induce interconversion of these isomeric and rotameric states on the NMR time scale,³⁴ with coalescence of the rotamers occurring at 340 K (DMSO-*d*₆). The upper temperature limit of the spectrometer prevented observation of complete coalescence of the remaining two isomeric signals, but peak convergence above 380 K strongly suggested that a single fully coalesced vinylic peak could be attained.

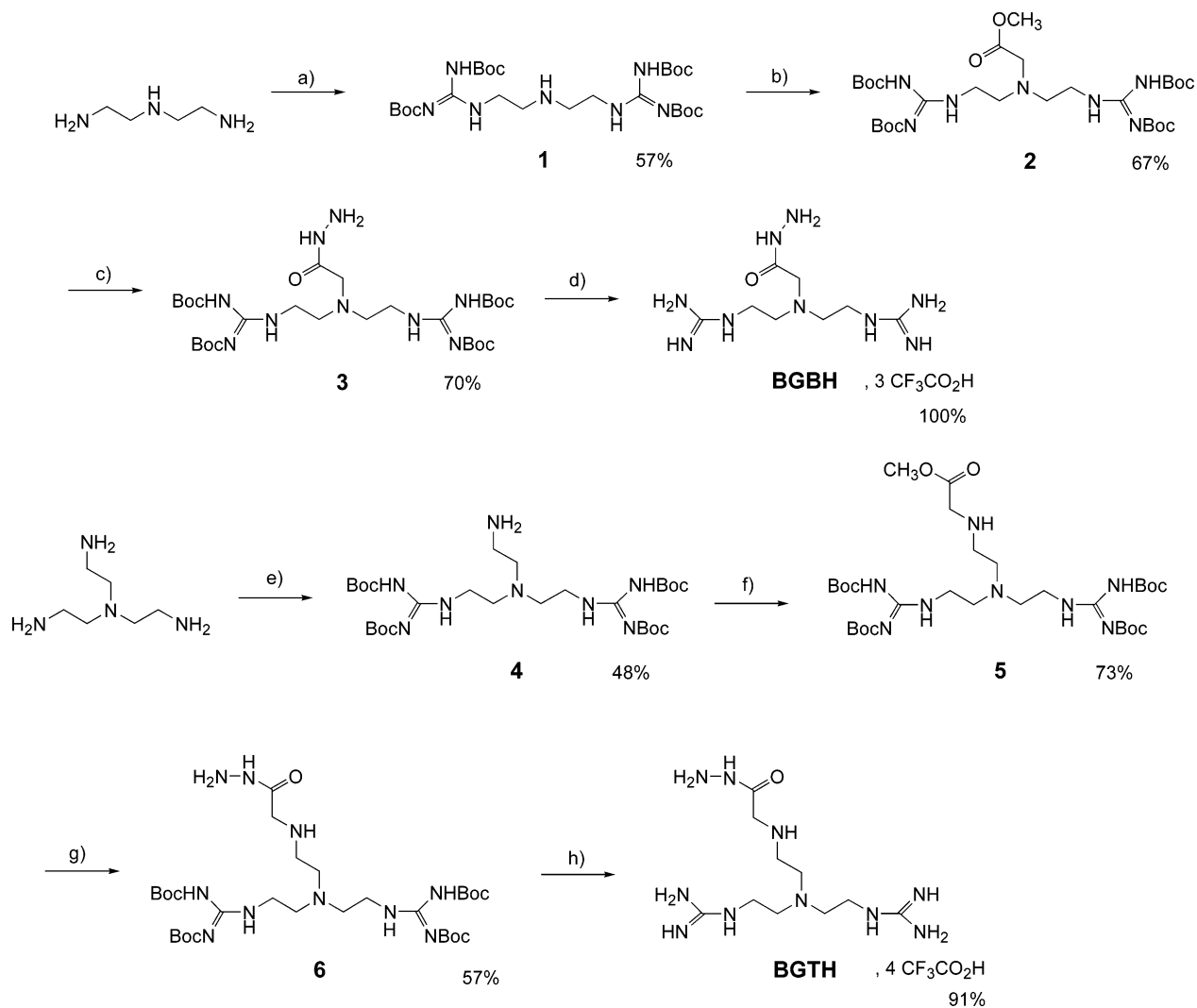


Figure 1. Synthesis of BGBH and BGTH bis-guanidinium acylhydrazines. Conditions and reagents are the following: (a) *N,N*-bis(*tert*-butoxycarbonyl)-1*H*-pyrazole-1-carboxamide, triethylamine, dioxane; (b) methyl chloroacetate, potassium iodide, potassium carbonate, acetonitrile; (c) hydrazine monohydrate, methanol; (d) trifluoroacetic acid, dichloromethane; (e) 1,3-bis(*tert*-butoxycarbonyl)-2-methyl-2-thiopseudourea, triethylamine, dioxane; (f) methyl bromoacetate, potassium iodide, potassium carbonate, acetonitrile; (g) hydrazine monohydrate, methanol; (h) trifluoroacetic acid, dichloromethane.

Hydrolysis Kinetic Analysis. To confirm the acid sensitivity of the integrated acylhydrazone function to hydrolysis, UV spectroscopy thermostated at 25 °C was used to monitor the integrity of the C=N hydrazone double bond over a period of 24 h. Cationic steroid hydrazones were dissolved in buffered aqueous solutions chosen to mimic the extremes of pH expected to exist in the cellular endosomal compartment (pH 7.2 and pH 4.8). The profiles in Figure 4 confirmed the increased rate of hydrolysis of the acylhydrazone group in acidic medium but more significantly allowed a comparison of the hydrolysis rates of the four different vectors. Clearly, the presence of an unsaturation at C-4 of BGBH-cholest-4-enone (half-lives of 10.4 days at pH 7.2 and 1.9 days at pH 4.8) and BGTH-cholest-4-enone (half-lives of 9.3 days at pH 7.2 and 2.3 days at pH 4.8) retarded their rate of cleavage compared to their saturated homologues BGBH-cholestanone (half-lives of 2.5 days at pH 7.2 and approximately 1.2 days at pH 4.8) and BGTH-cholestanone (half-lives of 3.4 days at pH 7.2 and approximately 1.3 days at pH 4.8), respectively. These findings are in agreement with previous work showing that the presence of a double bond

conjugated to the C=N hydrazone double bond plays a major role in the stability of steroid hydrazones³⁵ and highlights the fact that the vector structure has a direct influence on the sensitivity of its acylhydrazone linker to acidic pH. It is noteworthy here that although BGTC could not be tested in a similar manner (because of the absence of a C=N double bond), its linking carbamoyl bond is considered significantly more stable in acidic medium than the acylhydrazone bond.³⁶

In Vitro Transfection Activity of the Reagents in Aqueous Solution. Because lipofection involves the formation of lipid/DNA complexes, we first performed agarose gel electrophoresis experiments to assess DNA condensation by the acylhydrazone vectors. Representative results are shown in Figure 5. Plasmid DNA was completely retarded when complexed with the cholest-4-enone vectors (at lipid/DNA charge ratios of 3.9 and 6.7 for BGBH-cholest-4-enone and BGTH-cholest-4-enone, respectively), a finding indicative of the formation of stable DNA complexes. In contrast, plasmid DNA remained detectable at a lipid/DNA charge ratio of 6.7 in the case of the cholestanone vectors and even at very high charge ratios in the case of BGBH-cholestanone

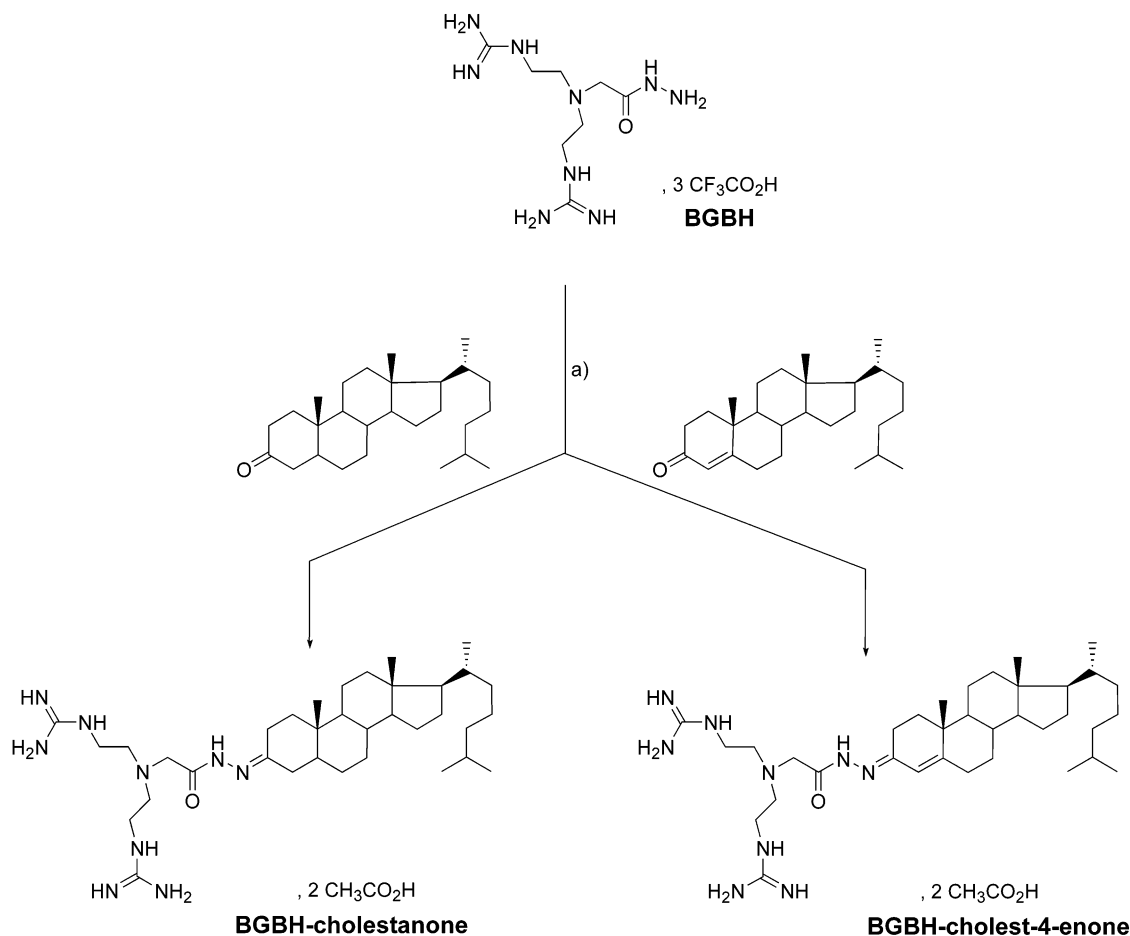


Figure 2. Synthesis of acylhydrazone cationic lipids BGBH-cholestanone and BGBH-cholest-4-enone. Conditions and reagents are the following: (a) acetic acid, methanol.

(Figure 5 and data not shown). When taking into account the hydrolysis kinetics data (see above), these findings are probably related to the lesser stability of the hydrazone bond in the saturated cholestanone vectors but are somewhat surprising when considering the actual observed half-lives of the cholestanone derived vectors at neutral pH. It should, however, be stressed here that whereas the hydrolysis kinetic data were obtained with vectors not complexed with DNA, the complexation of the vector to the DNA phosphates will alter the pK_a of not only the binding guanidinium groups but quite probably also of the hydrolysis-sensitive hydrazone bond (the pK_a difference depending on the strength of the binding). The resulting effective pK_a values are expected to be much higher and so may cause an accelerated hydrolysis of the vectors following complexation with the DNA because hydrazone hydrolysis requires protonation of the nitrogen as the first step.³⁷ Thus, it is the comparative rates (rather than the absolute rates) of hydrolysis of the series of vectors that should be the focus of attention when considering the stability profiles observed in the absence of DNA. Of note, monitoring of the hydrolysis of the vectors could not be conducted in the presence of plasmid because of the ubiquity of C=N double bonds in DNA.

Because all four vectors were found to be soluble in aqueous medium, a property likely related to the hydrophilicity of the guanidinium headgroups, we first investigated their usefulness as transfection reagents

by direct mixing with the DNA. Thus, *in vitro* transfection experiments were performed with HEK 293, COS, and HeLa cells, three cell lines commonly used in the laboratory. Here, because gene transfer by cationic lipids is presumed to involve electrostatic interactions between positively charged lipoplexes and negative cell surface residues, we examined the influence of the lipoplex charge ratio on transfection in order to determine the highest activity of the lipid/DNA aggregates (Figure 6). For all three cell lines, the saturated BGBH-cholestanone and BGTH-cholestanone vectors mediated no (or very low) transfection activity. In contrast, as shown by the representative dose response curves in Figure 6, the unsaturated vector BGBH-cholest-4-enone clearly yielded very high transfection levels for all three cell lines (with values up to 10^7 luciferase RLU/mg protein), whereas the unsaturated BGTH derivative mediated intermediate but significant gene transfection. This difference in transfection activity between the two unsaturated vectors will be discussed below. Here, as concerns the bell-shaped curves observed with BGBH-cholest-4-enone, we presume that the low transfection efficiency at low charge ratios may be due to reduced cell membrane binding. On the other hand, our previous studies with BGTC-based formulations,⁴ guanidylated polymerizable diacetylene lipids³⁸ and aminoglycoside-derived lipids,³⁹ and studies conducted by others on further cationic lipids suggest that the decrease in transfection activity at high charge ratio may reflect toxic effects of the cationic lipid.⁴⁰

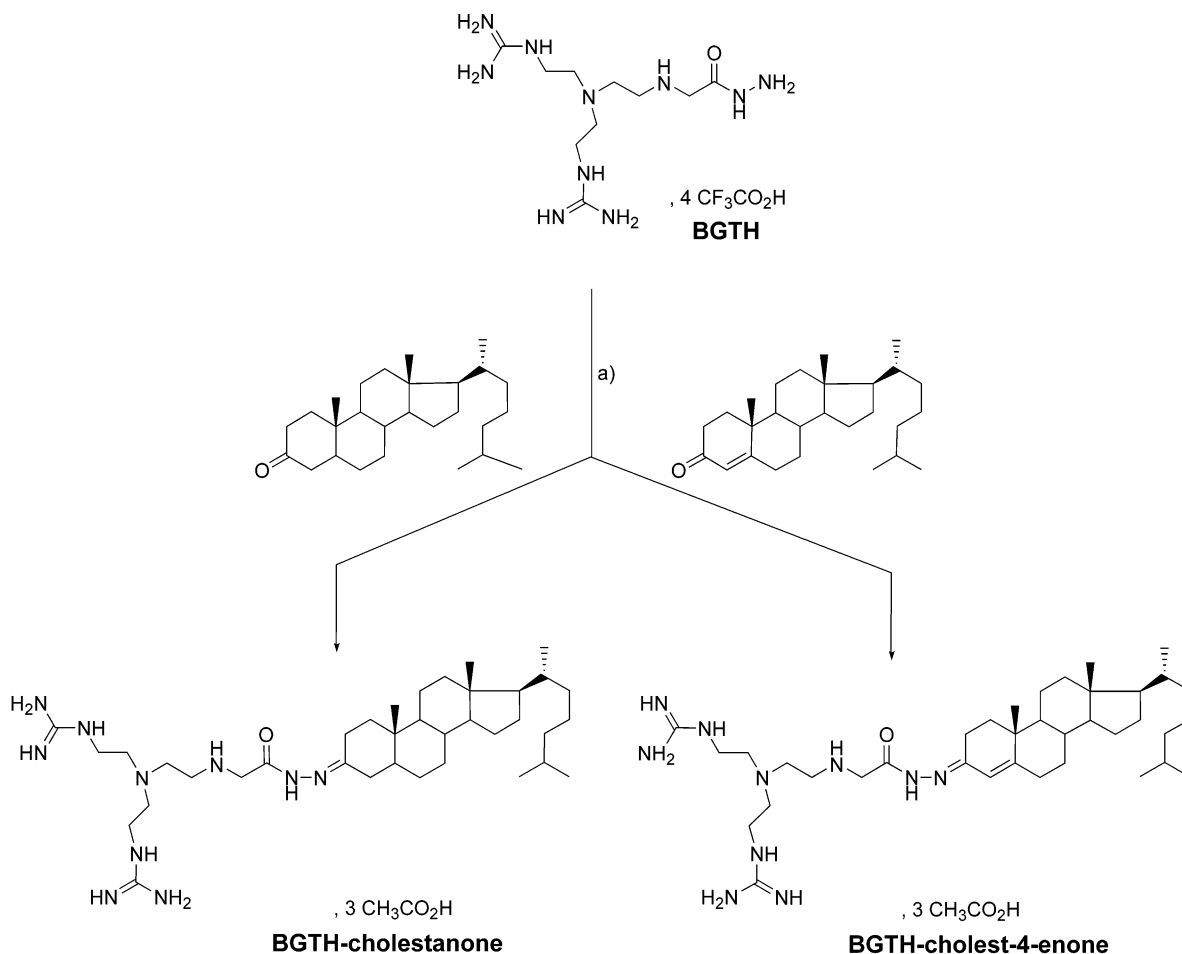


Figure 3. Synthesis of acylhydrazone cationic lipids BGTH-cholestanone and BGTH-cholest-4-enone. Conditions and reagents are the following: (a) acetic acid, methanol.

In Vitro Transfection Activity of BGBH-cholest-4-enone/DOPE Liposomes. Because the above in vitro dose response curves clearly indicated that BGBH-cholest-4-enone was the most efficient, we next performed a series of studies with BGBH-cholest-4-enone formulations in order to further assess their transfection properties (transfection experiments with BGBH-cholest-4-enone/DOPE liposomes, cytotoxicity studies, lipoplex size determination, in vivo transfection, and cytoplasmic expression studies).

Thus, we first prepared BGBH-cholest-4-enone/DOPE (molar ratio 3/2) liposomes and compared their efficiency for gene transfection into a variety of mammalian cell lines with that of BGBH-cholest-4-enone used alone. Indeed, cationic lipids are often formulated as liposomes with the neutral helper lipid DOPE because it is generally agreed that liposomes enriched with DOPE can exhibit a marked increase in transfection activity.^{1,41} In particular, Zhou and Huang have previously reported that because of the known fusogenic properties of DOPE, lipoplexes containing this colipid could better destabilize the endosomal membrane and facilitate escape into the cytosol.⁴² In these experiments we also tested for comparative purposes the transfection activity of BGTC/DOPE (molar ratio 3/2) liposomes. Although BGTC (whose structure is shown in Figure 7a) may not be the ideal non-hydrolyzable reference by which to study the effect of the inclusion of the acylhydrazone bond on transfection activity, preparation of a

closer relative posed a significant synthetic challenge. Indeed, reduction of the C=N double bond of BGBH-cholest-4-enone using conventional reducing agents led to inseparable mixtures of partially and over-reduced compounds.

As shown in Figure 7b, inclusion of the helper lipid DOPE in BGBH-cholest-4-enone formulations had a cell-type-dependent effect on the transfection efficiency. This is not surprising because several groups have reported that the efficiency of transfection mediated by mixtures of cationic lipids and helper lipids varies widely.^{1,2} Here, inclusion of DOPE had no significant effect with HEK 293, HeLa, and MITC cells, which are relatively easy to transfect. Interestingly, the A549 cell line, which was barely susceptible to transfection with BGBH-cholest-4-enone alone in aqueous solution, showed a significant increase in transfection levels on coformulation with DOPE. This is in agreement with the fact that the helper effect of DOPE is generally of particular importance with cells known to be intrinsically difficult to transfect. Consequently, because A549 cells are derived from a human lung carcinoma, we used BGBH-cholest-4-enone/DOPE liposomes for transfection of the mouse airways in vivo (see below). Finally, the results shown in Figure 7b also indicate that BGBH-cholest-4-enone/DOPE liposomes were slightly less efficient than BGTC/DOPE liposomes in particular with A549 lung cells. This finding, which suggests that the transfection activities of BGBH-

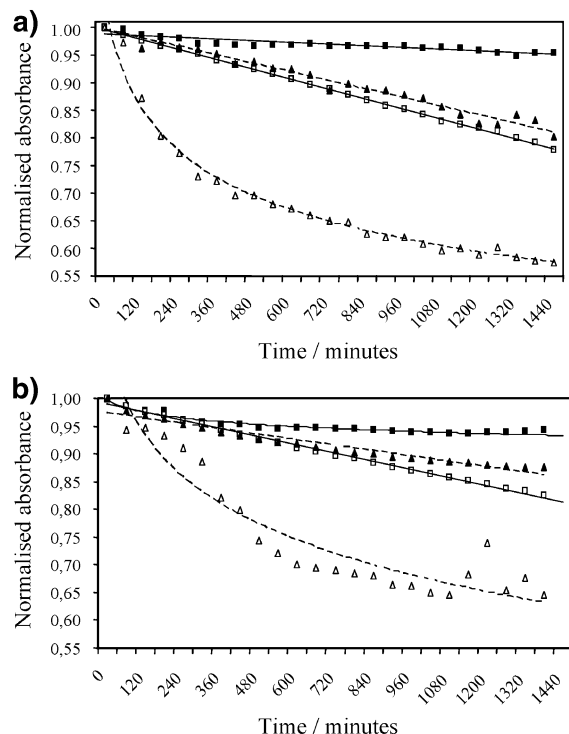


Figure 4. Analysis of the stability over 24 h of the four acylhydrazone-based cationic lipids at different pH values using UV absorbance to monitor the integrity of the hydrazone C=N double bond (filled plot points, pH 7.2; open plot points, pH 4.8): (a) UV absorbance at λ_{\max} (nm) of solutions of lipids BGBH-cholest-4-enone (square symbols, 272 nm at pH 7.2 and 275 nm at pH 4.8) and BGBH-cholestanone (triangular symbols, 235 nm at pH 7.2 and 237 nm at pH 4.8); (b) UV absorbance at λ_{\max} (nm) of solutions of lipids BGTH-cholest-4-enone (square symbols, 272 nm at pH 7.2 and 270 nm at pH 4.8) and BGTH-cholestanone (triangular symbols, 233 nm at pH 7.2 and 238 nm at pH 4.8).

cholest-4-enone liposomes and BGTC liposomes are of the same order of magnitude, will be discussed below because a somewhat similar observation was made in *in vivo* experiments of gene transfection into the mouse airways (see below).

In Vitro Cytotoxicity of BGBH-cholest-4-enone.

Because of the aforementioned possible toxic effects at high BGBH-cholest-4-enone/DNA ratio (see above and Figure 6), we also examined the cytotoxicity of the BGBH-cholest-4-enone formulations. Cytotoxicity was conveniently quantified by taking the total amount of cell protein in the cell lysate per well as an index of cell number. When using BGBH-cholest-4-enone alone in aqueous solution, cytotoxicity increased as the amount of cationic lipid increased, as shown in Figure 8a by the decline in total extractable cell protein at high charge ratios. Thus, the decline in transfection activity observed at high charge ratios was probably related to some toxicity of the reagent BGBH-cholest-4-enone. It is noteworthy that optimal *in vitro* transfection was achieved (see Figure 6) when using BGBH-cholest-4-enone lipoplexes with charge ratios (approximately 3.0) that led to minimal cytotoxicity. Such a low cytotoxicity may be due to the degradability of the hydrazone linker which could facilitate catabolism of the vector within the cell. This was further supported by a comparison of the cytotoxicity of BGBH-cholest-4-enone/DOPE liposomes and BGTC/DOPE liposomes over a range of cell

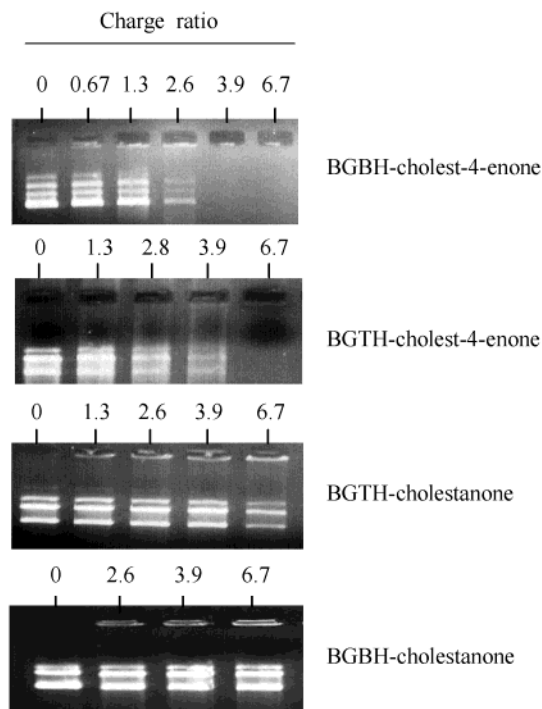


Figure 5. DNA binding by the acylhydrazone reagents. Agarose gel retardation (0.8%) of mixtures of pCMV-Luc plasmid with each of the synthesized acylhydrazone lipids, BGBH-cholestanone, BGBH-cholest-4-enone, BGTH-cholestanone, and BGTH-cholest-4-enone are represented as a function of lipid/DNA charge ratio (indicated above the lanes).

lines which showed that the hydrazone vector had in general a reduced toxicity compared to the nontriggerable reference (Figure 8b). Of note, inclusion of DOPE seemed in fact to reduce the toxicity of the BGBH-cholest-4-enone vector.

Size Determination of the Bioassemblies Formed by BGBH-cholest-4-enone.

BGBH-cholest-4-enone formulations (alone in aqueous medium and as liposomes with the neutral helper lipid DOPE) as well as BGBH-cholest-4-enone/DNA and BGBH-cholest-4-enone/DOPE/DNA lipoplexes were analyzed by dynamic light scattering. The results shown in Table 1 indicate that BGBH-cholest-4-enone alone formed polydisperse aggregates much larger than the corresponding liposomes and lipoplexes. Also, the lipoplexes prepared from liposomes were found to be generally larger than those prepared by simple mixing of vector and DNA. Analysis of the species formed by control BGTC formulations showed similar trends (Table 1). Interestingly, regardless of whether DOPE is included or not, lipoplexes formed from BGTC appeared to be smaller than those formed from BGBH-cholest-4-enone. These findings may be explained by a modification of the packing of the vector in the liposomes and lipoplexes due to the presence of the various isomers and rotamers seen in the cholestanone derivative (see above). Of note, the size of the lipoplexes formed by the acylhydrazone vector was found to increase on a prolonged time scale (≥ 1 day). This is likely due to their intrinsic lability properties because the size of the nonlabile BGTC lipoplexes remained invariable over a period of several days (data not shown). These results invite further investigation of the structural features formed by the BGBH-cholest-4-enone formulations (electron microscopy studies, X-ray

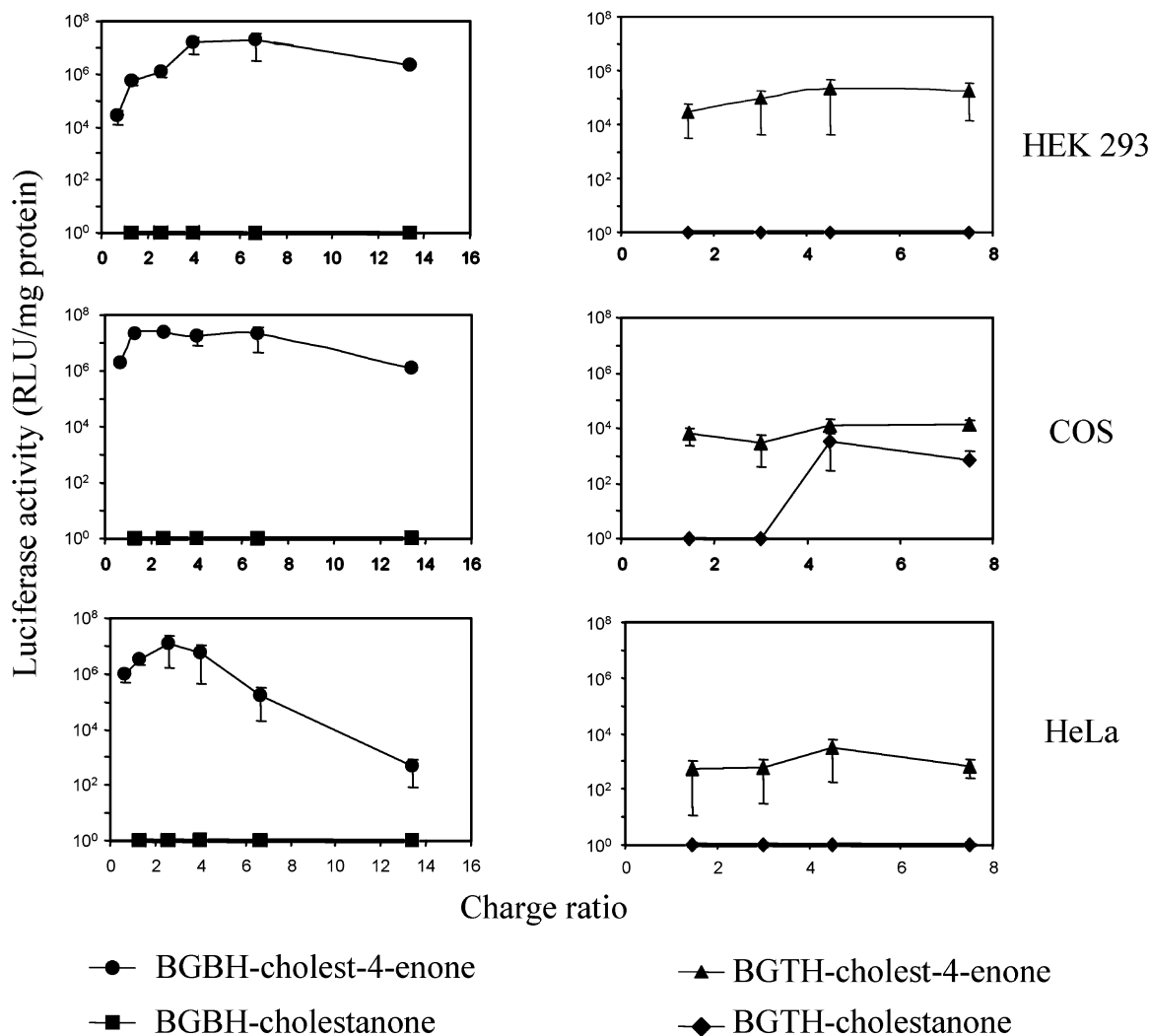


Figure 6. Dose response curves of in vitro transfection activity of reagents BGBH-cholest-4-enone (circles), BGBH-cholestanone (squares), BGTH-cholest-4-enone (triangles), and BGTH-cholestanone (diamonds). Luciferase reporter gene expression is indicated as a function of the charge ratio of the lipoplexes. HEK 293 cells, COS cells, and HeLa cells were transfected as described in the Experimental Section using lipoplexes prepared by mixing 5 μ g of luciferase-expressing plasmid DNA with the required amounts of lipid. Data are expressed as relative light units/mg cell protein (mean \pm SD with $n \geq 3$).

scattering experiments) as we have previously reported for BGTC-based formulations.⁴³

Effect of Serum on in Vitro Transfection by BGBH-cholest-4-enone/DOPE Liposomes. To get some insight into the potential of BGBH-cholest-4-enone for systemic in vivo gene delivery, we examined the effect of serum on in vitro gene transfection. Indeed, it has been reported that the presence of serum in the medium can alter the rate, extent, and mode of interaction of lipids or liposomes with cells.⁴⁴ Thus, we performed a series of comparative experiments in which HeLa cells were transfected by BGBH-cholest-4-enone/DOPE/pCMV-Luc lipoplexes (with charge ratios of 0.7, 2.0, and 3.9) in the presence and absence of 10% fetal calf serum. As indicated in Table 2, the presence of serum did not affect the activity of lipoplexes characterized by a charge ratio of 0.7 and reduced the efficiency of lipoplexes with a charge ratio of 2.0 by a factor of 2. There was even a more significant decrease in transfection when lipoplexes with a charge ratio of around 3.9 were used in the presence of serum. This may be explained by the fact that, in contrast to neutral lipoplexes, clearly positive lipoplexes may interact with

the negatively charged serum proteins. Of note, it has been reported that increasing the charge ratio of cationic liposomes can overcome the inhibitory effect of serum on lipofection.⁴⁵

In Vivo Gene Transfection into Mouse Airways. Because we have previously reported that BGTC/DOPE liposomes can mediate efficient gene transfection into the mouse airways,^{5,6} we investigated the potential of BGBH-cholest-4-enone/DOPE liposomes for lung-directed gene transfer in vivo. In these experiments, colloidal stable BGBH-cholest-4-enone/DOPE lipoplexes carrying the CAT-expressing plasmid pCIK-CAT were prepared and administered via intranasal instillation as previously described.^{6,39} Schematically, concentrated solutions (characterized by a DNA concentration of about 0.6 mg/mL) of colloidal stable lipoplexes (with a positive charge ratio of 3.2) were obtained by addition of the steric stabilizer cholesterol-poly(ethylene glycol) (Chol-PEG) to the BGBH-cholest-4-enone/DOPE liposomes prior to their mixing with the DNA (final Chol-PEG/DNA w/w ratio of 2). Indeed, we have previously reported that the use of the Chol-PEG conjugate (where a PEG chain of approximately 100

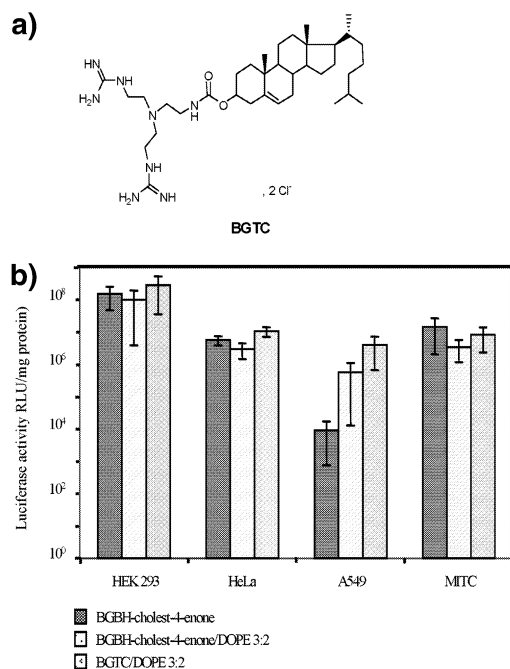


Figure 7. (a) Structure of the cationic lipid BGTC. (b) Luciferase expression in various mammalian cell lines transfected by BGBH-cholest-4-enone lipoplexes or BGBH-cholest-4-enone/DOPE lipoplexes (at optimal charge ratios of 2.6–3.9), with BGTC/DOPE lipoplexes (at optimal charge ratio of 3.9) as reference. The various mammalian cell lines were transfected as described in the Experimental Section by mixing luciferase-expressing plasmid DNA (5 μ g) with the required amounts of lipid. Data are expressed as relative light units/mg cell protein (mean \pm SD with $n \geq 3$).

oxyethylene units is linked to a cholesterol anchor) allows preparation of concentrated, colloidal stable BGTC/DOPE lipoplexes that can mediate gene transfection into the mouse airways via intranasal administration.⁶ Thus, at 48 h after dosing, the lungs and tracheas were separately removed from the treated mice and assayed for CAT expression. Significant CAT expression was obtained in the lung homogenates because the observed CAT levels were much higher than those obtained in control mice receiving an identical dose of “naked” (uncomplexed) pCIK-CAT plasmid (Table 3), the increase in CAT expression observed with BGBH-cholest-4-enone-based lipoplexes being statistically significant (p value of 0.018) when comparing the CAT levels obtained with BGBH-cholest-4-enone/DOPE lipoplexes with those obtained with naked DNA. Thus, under our conditions, BGBH-cholest-4-enone/DOPE liposomes can mediate efficient gene transfection into the mouse lung in vivo. Much lower CAT levels were observed in the trachea than in the lung homogenates (data not shown), which is in agreement with our previous work with BGTC-based lipoplexes.⁶ We have indeed previously found that BGTC-based lipoplexes could mediate levels of CAT expression of the same order of magnitude as those obtained here with BGBH-cholest-4-enone-based lipoplexes. In our opinion, the fact that the BGBH-cholest-4-enone hydrazone vector used herein does not perform better than the nontriggerable BGTC vector does not undermine the soundness of our approach. Indeed, when considering the highly complex series of steps underlying gene transfer, it should be stressed that the hydrazone vector may make use of

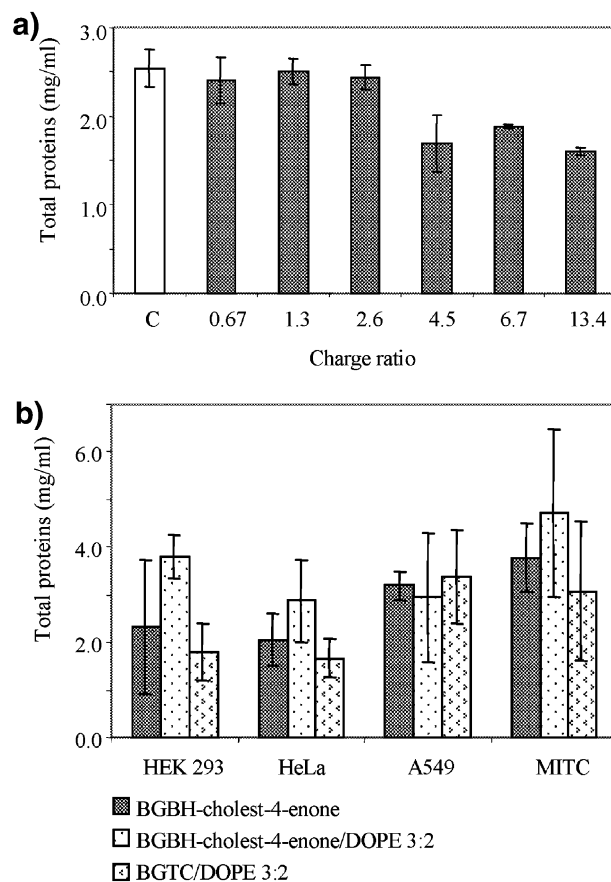


Figure 8. (a) Cytotoxicity of reagent BGBH-cholest-4-enone with HeLa cells. Cells were transfected as described in the Experimental Section using plasmid DNA (5 μ g) mixed with the amounts of lipids required to form lipoplexes characterized by the indicated charge ratios. At 48 h post-transfection, cells were harvested for monitoring of the luciferase expression, and toxicity was quantified using the total amount of cell protein in cell lysate as an index of cell number, cell death leading to a decrease in extractable protein (C, control untransfected cells). Data are expressed as concentration of extractable cell protein in the cell lysate (fixed volume) (representative experiment, mean \pm SD with $n = 3$). (b) Cytotoxicity in various mammalian cell lines transfected by BGBH-cholest-4-enone lipoplexes or BGBH-cholest-4-enone/DOPE lipoplexes (at charge ratios of 2.6–3.9), with BGTC/DOPE lipoplexes (at a charge ratio of 3.9) as reference. Data are expressed as the concentration of extractable cell protein in the cell lysate (fixed volume) (mean \pm SD with $n \geq 3$).

Table 1. Dynamic Light Scattering Analysis of BGBH-cholest-4-enone and BGTC Alone, Formulated as Liposomes with DOPE and as Lipoplexes with or without DOPE (with a Positive Charge Ratio of 6.0) in Buffered Solution (Hepes 20 mM)

formulation	size distribution (nm)	comments
BGBH-cholest-4-enone	698 \pm 193	polydisperse
BGTC	287 \pm 70	polydisperse
BGBH-cholest-4-enone/DOPE	90 \pm 30	monodisperse
BGTC/DOPE	56 \pm 19	monodisperse
BGBH-cholest-4-enone/DNA	161 \pm 19, 393 \pm 188	polydisperse
BGTC/DNA	32 \pm 11	monodisperse
BGBH-cholest-4-enone/ DOPE/DNA	382 \pm 148	polydisperse
BGTC/DOPE/DNA	83 \pm 32	monodisperse

specific mechanisms to overcome the barriers encountered (see below). Thus, BGBH-cholest-4-enone-based

Table 2. Effect of Serum on Luciferase Gene Activity in HeLa Cells^a

charge ratio (\pm)	without serum	with 10% serum
0.7	$1.18 \times 10^6 (\pm 3.68 \times 10^5)$	$1.21 \times 10^6 (\pm 5.63 \times 10^5)$
2.0	$1.39 \times 10^7 (\pm 1.77 \times 10^6)$	$5.48 \times 10^6 (\pm 8.41 \times 10^5)$
3.9	$4.38 \times 10^6 (\pm 3.31 \times 10^6)$	$6.48 \times 10^5 (\pm 6.03 \times 10^5)$

^a BGBH-cholest-4-enone/DOPE/DNA lipoplexes at charge ratios of 0.7, 2.0, or 3.9 were first prepared in a total volume of 100 μ L of FCS-free DMEM for 30 min, and then an amount of 400 μ L of DMEM with or without 10% FCS was added to the transfection medium just prior incubation with the cells. The level of luciferase gene expression was evaluated as described in the Experimental Section. Data are expressed as relative light units RLU/mg cell protein (mean \pm SD with $n \geq 3$).

Table 3. In Vivo Gene Transfection into Mouse Airways^a

type of vector	CAT expression in lungs (ng/100 mg protein)
"naked" DNA	0.15 ± 0.16
BGBH-cholest-4-enone/DOPE	2.69 ± 2.06

^a Chol-PEG-stabilized BGBH-cholest-4-enone/DOPE/DNA lipoplexes (characterized by a charge ratio of 3.2 and a Chol-PEG/DNA (w/w) ratio of 2) were used to deliver a total dose of 100 μ g of CAT-expressing plasmid DNA. Intranasal instillation was performed, and lungs of the treated mice were harvested, processed, and assayed for CAT expression as described in the Experimental Section. Data are expressed as nanograms of CAT protein per 100 mg of total cell protein (mean \pm SD with $n = 11$ for BGBH-cholest-4-enone/DOPE liposomes), the increase in CAT expression by BGBH-cholest-4-enone-based lipoplexes being statistically significant ($p = 0.018$) when comparing the CAT levels obtained with BGBH-cholest-4-enone lipoplexes with those obtained with "naked" DNA.

formulations in particular, and hydrazone-based formulations in general, may be promising candidates for further development with a view to lung-directed gene therapy (for diseases such as cystic fibrosis) and possibly other in vivo gene therapy applications.

Cytoplasmic Expression To Assess Endosomal Release of DNA. To understand further the mechanisms of BGBH-cholest-4-enone-mediated lipofection,

we studied cytoplasmic and nuclear luciferase gene expression in T7 RNA polymerase-expressing 293-T7 cells^{46,47} and compared the results to levels of gene expression achieved with BGTC as standard control vector. Such a direct comparison between a cytoplasmic and a nuclear expression system was an attempt at breaking down the process of transfection into a series of steps, highlighting in particular the rate of DNA release from the endosomal compartment to the cytosol. This was possible by comparing the transfection of either pT7-Luc (cytoplasmic expression) or pCMV-Luc (nuclear expression) plasmids into engineered 293-T7 cells where, in addition to normal nuclear transcription, there is cytoplasmic transcription of T7 promoter-driven genes because these cells express cytoplasmic T7 bacteriophage RNA polymerase. In other words, when the T7 RNA polymerase-based cytoplasmic expression system is used, transcription of a T7-driven transgene takes place independently of the nuclear transcriptional machinery, thus permitting direct studies of DNA delivery from endosomal compartments into the cytosol by excluding the nuclear uptake step.

The profiles of cytoplasmic and nuclear luciferase expression levels obtained with the BGBH-cholest-4-enone and BGTC vectors are shown as a function of time in Figure 9. First, at early time points (<2 h), the cytoplasmic expression levels were clearly much higher than the nuclear expression levels. This was expected because nuclear transcription occurs after cytoplasmic transcription because of the greater number of cellular barriers that have to be overcome before nuclear transcription can start. At these very early time points, cytoplasmic expression obtained with BGTC was actually higher (about 50-fold at 1 h) than that obtained when using BGBH-cholest-4-enone. Thus, BGTC appears to be more capable than BGBH-cholest-4-enone to promote escape of the DNA from early (only slightly acidic) endosomes. This may be related to a higher intrinsic endosomolytic activity of BGTC and/or to the

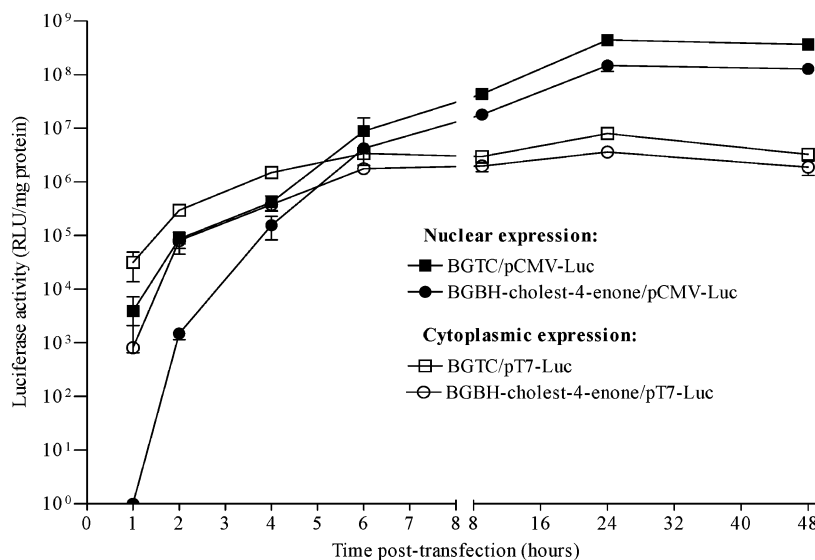


Figure 9. Time course of luciferase activity when using cytoplasmic and nuclear expression systems. HEK 293-T7 cells were transfected with lipoplexes (characterized by a charge ratio of 2.6) formed by mixing BGBH-cholest-4-enone (or control BGTC) with either pT7-Luc (cytoplasmic expression) or pCMV-Luc (nuclear expression) plasmid DNA. HEK 293-T7 is a cell line stably transfected with pCMV/T7-T7p α and producing endogenous T7 RNA polymerase. At the indicated time points post-transfection, the cells were harvested and luciferase activity was determined as described in the Experimental Section. Data for luciferase activity are expressed as relative light units (RLU)/mg cell protein (mean \pm SD with $n \geq 3$).

smaller size of BGTC/DNA lipoplexes (see above) because it is generally agreed that smaller lipoplexes are better taken up by cells via endocytosis. Accordingly, at early time points, nuclear expression was also higher with BGTC than with BGBH-cholest-4-enone, an almost 100-fold difference being observed at 2 h.

Second, Figure 9 also indicates that at intermediate time points (from 2 to 6 h) the nuclear expression levels increased more quickly than the cytoplasmic levels and became even slightly higher at 6 h. This again is in agreement with the fact that nuclear transcription occurs after cytoplasmic transcription. It is noteworthy that at these intermediate time points the difference in cytoplasmic expression levels between BGTC and BGBH-cholest-4-enone does significantly decrease, the difference in nuclear expression levels decreasing even more (from a 100-fold difference at 2 h to an approximately 5-fold difference at 6 h). These data strongly suggest that BGBH-cholest-4-enone is superior to BGTC in mediating cytoplasmic release of the DNA at time points along the endocytosis pathway which probably correspond to more acidic compartments than early endosomes. It is tempting to speculate that this may be related to the expected hydrolytic properties of BGBH-cholest-4-enone when the continuously decreasing pH in the endosome reaches a threshold whereupon plasmid release can occur to a significant degree.

Finally, at late time points (>6 h), nuclear expression largely overrides cytoplasmic expression, a 100-fold difference being observed at 24 h. This again is basically due to the occurrence of nuclear transcription after cytoplasmic transcription. It may, however, also be due in part to the fact that cytoplasmic expression may plateau because the quantity of T7 polymerase produced by the 293-T7 cells has been reported to be relatively low.⁴⁷ Finally, it should be stressed that at these late time points, the nuclear expression levels reached with BGBH-cholest-4-enone were only slightly lower than those observed with BGTC, with the large difference observed at early time points no longer maintained. In conclusion, taken together, these results suggest that the BGBH-cholest-4-enone vector is particularly efficient at intermediate time points along the endocytosis pathway, whereas the control BGTC vector seems to be more efficient for DNA escape from early endosomes.

Conclusions and Perspectives

With a view to exploiting the endocytosis pathway of lipofected DNA, which is characterized by a gradual decrease in pH, we have synthesized a family of guanidinium-based cationic steroid derivatives with an acid-sensitive acylhydrazone linker and examined their transfection properties. Our results show that one vector of our series, BGBH-cholest-4-enone, mediates efficient gene transfection into mammalian cells *in vitro* and further is capable of transfecting mouse airways *in vivo* when formulated as liposomes with DOPE. Importantly, BGBH-cholest-4-enone displayed relatively low cellular toxicity at the lipid/DNA ratio required for optimal *in vitro* transfection, a factor presumably due to its degradable acylhydrazone linker.

BGBH-cholest-4-enone is characterized by a double bond in the steroid ring A conjugated to a hydrazone carbon–nitrogen double bond. According to previous

work by others, it was probable that such double bond conjugation would play a role in the stability of the cationic lipids, the unsaturated BGBH-cholest-4-enone and BGTH-cholest-4-enone being expected to be more stable than the saturated BGBH-cholestanone and BGTH-cholestanone.³⁵ This correlation was borne out in the hydrolysis experiments where the unsaturated vectors were found to hydrolyze at a slower rate than the corresponding saturated vectors. The inability of the latter to complex DNA according to gel electrophoresis experiments is likely linked to their relative instability in aqueous solution. Transfection data provided the ultimate evidence that the saturated conjugates do not function as gene delivery vectors. Thus, these results strongly suggest that a window of stability of the acylhydrazone bond is required for efficient gene transfection. There was, however, a difference in transfection activity between the two unsaturated homologues, with BGBH-cholest-4-enone being clearly more efficient than BGTH-cholest-4-enone. This may be related to differences in the length of the spacer and/or in the number of cationic groups per molecule. Because an increase in positive charge is generally considered to be desirable for gene transfer, it may be hypothesized that it is the chain extension that is limiting in the case of BGTH-cholest-4-enone. However, within studies based on polyamine–steroid conjugates, transfection levels have been seen to drop on increase in both length and total charge of the vectors, the collapse in transfection ability being considered due to an increased flexibility of the headgroup of the longer compounds resulting in a more folded, rather than stretched, structure.⁴⁸

Taken together, the results presented herein shed some light on the structure–activity relationships of guanidinium-based cationic lipids with an acid-sensitive acylhydrazone bond. Important additional data for a better knowledge of these relationships might be obtained via transfection studies with other acylhydrazone lipids characterized by amine-based headgroups and/or a hydrophobic moiety consisting of aliphatic chains. On the other hand, although the hydrolysis kinetic studies confirmed the acid sensitivity of our acylhydrazones in the test tube and the cytoplasmic expression studies suggested that the presence of the acylhydrazone bond played an important role in the cellular trafficking of BGBH-cholest-4-enone lipoplexes, it will also be important to better understand the cellular and molecular mechanisms underlying transfection by acylhydrazone lipids. In particular, this may involve comparative studies on the subcellular trafficking of cytoplasmic and nuclear expression systems in the presence of cell-trafficking inhibitors (such as bafilomycin A, chloroquine, and nocodazole) as well as electron microscopy studies of transfected cells and fluorescence microscopy studies with labeled DNA and/or lipids. According to previous work on triggerable lipid vesicles,¹⁵ it may be expected that such studies should help to develop acylhydrazone cationic lipids with an acid sensitivity optimal for endosomal escape of the DNA and thus improve the transfection efficiency of such vectors. In conclusion, despite the fact that the hydrazone-based BGBH-cholest-4-enone vector investigated herein did not perform better than the stable BGTC control vector, it should be stressed that the present studies show that

incorporation of an acylhydrazone function into the cationic lipid structure allows a modulation of its transfection activity and that a pH-triggerable hydrazone-containing vector can mediate efficient gene transfection in vitro as well as in vivo. Thus, our work provides a basis for the exploration of a broad range of related gene delivery systems for gene transfer studies and gene therapy applications.

Experimental Section

Chemistry: Preparation and Characterization of Acylhydrazone Cationic Lipids. Materials and Analytical Methods. All commercially available chemicals were reagent grade and were used without further purification. Unless otherwise indicated, all the reactions were performed at room temperature. Flash chromatography employed Merck silica gel (Kieselgel 60 (0.040–0.063 mm)), and analytical TLC was performed with 0.2 mm silica-coated aluminum sheets, with visualization by UV light or by dipping in a solution of ninhydrin (0.3% in weight in *n*-butanol containing 3% acetic acid in volume). Melting points were determined on an Electrothermal 9100 apparatus, and ^1H and ^{13}C NMR spectra were recorded on a Bruker Avance 300 spectrometer. MALDI/TOF mass spectra were recorded with a PerSeptive Biosystems Voyager Elite (Framingham, MA) time-of-flight mass spectrometer (Université Pierre et Marie Curie, Paris, France). IR spectra were obtained on a Bruker Vector 22 FT-IR spectrometer, and the microanalyses were performed at the Service de Microanalyse (Université Pierre et Marie Curie, Paris, France). Target compounds were designed to be cleavable and as such unavoidably coexisted with a minute fraction of partially hydrolyzed material caused by the action of atmospheric humidity and their hygroscopic nature. Accordingly, all target compounds were submitted to high-resolution mass spectrometry analysis because the obtention of an accurate elemental analysis would have been prevented by the presence of hydrolyzed material (cholesterol and BGTG or BGBH). High-resolution mass spectrometry was conducted using positive fast atomic bombardment (JEOL MS700, with Magic Bullet matrix) at the Service de Spectrométrie de Masse (Ecole Normale Supérieure, Paris, France).

Synthesis of the Bis-guanidinium Acylhydrazone BGBH. Synthesis of *N,N'*-Bis[*N,N*-bis-*tert*-butoxycarbonylguanyl] Diethylenetriamine. Compound 1 (Figure 1). *N,N*-Bis(*tert*-butoxycarbonyl)-1*H*-pyrazole-1-carboxamide (2.00 g, 6.45 mmol) was added to a solution of diethylenetriamine (0.35 mL, 3.22 mmol) in dioxane (80 mL), which was subsequently placed under an atmosphere of nitrogen. After 5 min triethylamine (0.90 mL, 6.45 mmol) was added dropwise, and the solution was left to stir overnight. The total consumption of *N,N*-bis(*tert*-butoxycarbonyl)-1*H*-pyrazole-1-carboxamide was checked by TLC (CH_2Cl_2). The solvent was evaporated under vacuum, and the residue was dissolved in dichloromethane before washing four times with water. The solvent was dried over MgSO_4 and again removed in vacuo. The product was isolated by chromatography on silica gel ($\text{CH}_2\text{Cl}_2/\text{MeOH}$, 98:2) as a white foam (0.909 g, 48%). ^1H NMR (200 MHz, CD_3OD) (TMS) δ 3.56 (m, 4H, CH_2), 3.01 (m, 4H, CH_2), 1.51 (s, 18H, $\text{C}(\text{CH}_3)_3$), 1.45 (s, 18H, $\text{C}(\text{CH}_3)_3$); ^{13}C NMR (50 MHz, CDCl_3) (TMS) δ 162.77 (CO), 155.52 (CN), 152.31 (CO Boc), 82.16, 78.33 ($\text{C}(\text{CH}_3)_3$), 47.14 (CH_2), 40.08 (CH_2), 27.36 ($\text{C}(\text{CH}_3)_3$); IR (cm^{-1}) 3335, 2979, 2933, 1724, 1641. Anal. ($\text{C}_{26}\text{H}_{49}\text{N}_7\text{O}_8$) C, H, N. MS (m/z) [$\text{M} + \text{H}$] $^+$ 588.

Synthesis of *N,N'*-Bis[*N,N*-bis-*tert*-butoxycarbonylguanyl]-*N'*-methyl Acetate Diethylenetriamine. Compound 2 (Figure 1). Compound 1 (100 mg, 170 μmol), potassium carbonate (50 mg, 362 μmol), and potassium iodide (10 mg, 60 μmol) were dissolved in acetonitrile (2 mL), to which was added dropwise methyl chloroacetate (15 μL , 170 μmol). The mixture was left to stir overnight upon which the solvent was evaporated off in vacuo, and the product was isolated by chromatography on silica gel ($\text{CH}_2\text{Cl}_2/\text{MeOH}$, 99:1) as a white foam (75 mg, 67%). ^1H NMR (200 MHz, CD_3OD) (TMS) δ 3.69

(s, 3H, OCH_3), 3.54 (s, 2H, CH_2CO), 3.40 (m, 4H, CH_2), 2.88 (m, 4H, CH_2), 1.50 (s, 18H, $\text{C}(\text{CH}_3)_3$), 1.46 (s, 18H, $\text{C}(\text{CH}_3)_3$); ^{13}C NMR (50 MHz, CDCl_3) (TMS) δ 71.20 (CO), 163.27 (CN), 155.90, 152.72 (CO Boc), 82.51, 78.70 ($\text{C}(\text{CH}_3)_3$), 54.40 (CH_2CO), 53.02, 39.26 (CH_2), 51.08 (OCH_3), 28.11, 27.87 ($\text{C}(\text{CH}_3)_3$); IR (cm^{-1}) 3331, 2980, 2935, 1724, 1642. Anal. ($\text{C}_{29}\text{H}_{53}\text{N}_7\text{O}_{10}$) C, H, N. MS (m/z) [$\text{M} + \text{H}$] $^+$ 660.

Synthesis of *N,N'*-Bis[*N,N*-bis-*tert*-butoxycarbonylguanyl]-*N'*-acetylhydrazone Diethylenetriamine. Compound 3 (Figure 1). Compound 2 (118 mg, 0.18 mmol) was dissolved in a stirred solution of hydrazine monohydrate (2.6 mL, 53.57 mmol) and MeOH (10.4 mL). The consumption of starting material was confirmed by TLC after 19 h, and the solution was reduced under vacuum. The product was isolated by chromatography on silica gel ($\text{CH}_2\text{Cl}_2/\text{MeOH}$, 98:2) as a white foam (83 mg, 70%). ^1H NMR (300 MHz, CD_3OD) δ 3.49 (t, J5.7, 4H, CH_2), 3.31 (s, 2H, CH_2CO), 2.79, 2.90 (t, J5.7, 4H, CH_2), 1.54, 1.48 (s, 18H, $\text{C}(\text{CH}_3)_3$), 1.48 (s, 18H, $\text{C}(\text{CH}_3)_3$); ^{13}C NMR (50 MHz, CDCl_3) (TMS) δ 170.02 (CO), 162.93 (CN), 155.95, 153.23 (CO Boc), 83.26, 79.11 ($\text{C}(\text{CH}_3)_3$), 58.14 (CH_2CO), 53.69, 38.36 (CH_2), 28.15, 27.98 ($\text{C}(\text{CH}_3)_3$); IR (cm^{-1}) 3329, 2979, 1721, 1641, 1611. Anal. ($\text{C}_{28}\text{H}_{53}\text{N}_9\text{O}_9$) C, H, N. MS (m/z) [$\text{M} + \text{H}$] $^+$ 660.

Synthesis of the Trifluoroacetic Acid Salt of *N,N'*-Bis-guanyl-*N'*-acetylhydrazone Diethylenetriamine. Compound BGBH (Figure 1). Trifluoroacetic acid (4.19 mL, 54.87 mmol) was added dropwise to a solution of compound 3 (386 mg, 0.59 mmol) in dichloromethane (13 mL). The reaction mixture was left to stir for 16 h at room temperature upon which the excess trifluoroacetic acid was removed in vacuo. The residue was washed three times with dichloromethane and three times with hexane before evacuating, yielding the product as an oil (352 mg, 100%). ^1H NMR (300 MHz, D_2O) δ 4.05, 3.92 (s, 2H, CH_2CO), 3.50, 3.44 (t, J6.1, 4H, CH_2), 3.30, 3.20 (t, J6.1, 4H, CH_2); ^{13}C NMR (50 MHz, CD_3OD) (TMS) δ 165.00 (CO), 158.94 (CN), 57.03, 55.12, 54.75, 40.64 (CH_2); IR (cm^{-1}) 3341, 1676, 1586. MS (m/z) [$\text{M} + \text{H}$] $^+$ 260.

Synthesis of the Bis-guanidinium Acylhydrazone BGTG. Synthesis of *N,N'*-Bis[*N,N*-bis-*tert*-butoxycarbonylguanyl]-*N'*-aminoethyl Diethylenetriamine. Compound 4 (Figure 1). 1,3-Bis(*tert*-butoxycarbonyl)-2-methyl-2-thiopsedourea (2.328 g, 8 mmol), diisopropylethylamine (1.4 mL, 8 mmol), and tris(2-aminoethyl)amine (0.586 g, 4 mmol) were dissolved in dichloromethane (20 mL) and left to stir for 24 h. The total consumption of 1,3-bis(*tert*-butoxycarbonyl)-2-methyl-2-thiopsedourea was checked by TLC (CH_2Cl_2). The solution was washed three times with water and dried over MgSO_4 , and the solvent was removed in vacuo. The product was isolated by chromatography on silica gel (EtOAc/EtOH , 7:3) as a white foam (1.214 g, 48%). ^1H NMR (200 MHz, CDCl_3) δ 11.5 (t, 2H, NH/Boc), 8.6 (t, 2H, NH/CH_2), 3.5 (m, 4H, CH_2), 2.8 (m, 2H, CH_2NH_2), 2.6 (m, 6H, CH_2), 1.5 (s, 18H, $\text{C}(\text{CH}_3)_3$), 1.4 (s, 18H, $\text{C}(\text{CH}_3)_3$); ^{13}C NMR (75 MHz, CDCl_3) δ 163.54 (CN), 156.11, 153.12 (CO Boc), 82.99, 79.16 ($\text{C}(\text{CH}_3)_3$), 58.11, 53.35, 39.87, 38.99 (CH_2), 28.31, 28.08 ($\text{C}(\text{CH}_3)_3$). Anal. ($\text{C}_{28}\text{H}_{54}\text{N}_8\text{O}_8$) C, H, N. MS (m/z) [$\text{M} + \text{H}$] $^+$ 631, [$\text{M} + \text{Na}$] $^+$ 653, [$\text{M} + \text{H} - \text{Boc}$] $^+$ 531, [$\text{M} + \text{Na} - \text{Boc}$] $^+$ 553, [$\text{M} + \text{H} - 2\text{Boc}$] $^+$ 431, [$\text{M} + \text{Na} - 2\text{Boc}$] $^+$ 453.

Synthesis of *N,N'*-Bis[*N,N*-bis-*tert*-butoxycarbonylguanyl]-*N'*-[*N*-methylacetate(aminoethyl)] Diethylenetriamine. Compound 5 (Figure 1). Compound 4 (117 mg, 186 μmol), potassium carbonate (55 mg, 398 μmol), and potassium iodide (11 mg, 66 μmol) were dissolved in acetonitrile (2 mL), and the mixture was cooled over an ice bath. Methyl bromoacetate (18 μL , 190 μmol) was added dropwise to the mixture, which was left to stir for 19 h. The solvent was evaporated in vacuo, and the product was isolated by chromatography on silica gel ($\text{CH}_2\text{Cl}_2/\text{MeOH}$, 98:2) as a white foam (95 mg, 73%). ^1H NMR (300 MHz, CDCl_3) δ 8.59 (m, 2H, NH/C), 3.76 (s, 3H, OCH_3), 3.53–3.41 (m, 6H, CH_2), 2.70–2.64 (m, 8H, CH_2), 2.12 (br s, $\text{NH/CH}_2\text{O}$), 1.46, 1.43 (s, 36H, $\text{C}(\text{CH}_3)_3$); ^{13}C NMR (75 MHz, CD_3OD) δ 172.13 (CO), 163.12 (CN), 156.04, 152.82 (CO Boc), 82.92, 78.32 ($\text{C}(\text{CH}_3)_3$), 53.88

(CH₂CO), 52.79, 50.81, 46.19, 39.00 (CH₂), 49.32 (OCH₃), 27.20, 26.98 (C(CH₃)₃); MS (*m/z*) [M + H]⁺ 703.

Synthesis of *N*¹,*N*⁷-Bis[*N,N*-bis(*tert*-butoxycarbonyl)guananyl]-*N*¹-[*N*-acetylhydrazone(aminoethyl)] Diethylenetriamine. Compound 6 (Figure 1). Compound 5 (28 mg, 40 μmol) was added to a stirred solution of hydrazine monohydrate (116 μL, 2.39 mmol) and MeOH (220 μL). The consumption of starting material was confirmed by TLC after 2 h, and the solution was reduced under vacuum. The product was isolated by chromatography on silica gel (CH₂Cl₂/MeOH, 96:4) as a white foam (16 mg, 57%). ¹H NMR (300 MHz, CDCl₃) δ 8.56 (br s, 2H, NH), 8.38 (br s, 1H, NH), 3.85 (br s, 2H, NH), 3.53 (m, 4H, CH₂), 3.38 (s, 2H, CH₂CO), 2.69 (m, 8H, CH₂), 1.53, 1.50 (s, 36H, C(CH₃)₃); ¹³C NMR (75 MHz, CDCl₃) δ 171.95 (CO), 163.51 (CN), 156.07, 153.25 (CO Boc), 83.11, 79.26 (C(CH₃)₃), 54.53 (CH₂CO), 53.12, 51.73, 47.64, 38.85 (CH₂), 28.30, 28.08 (C(CH₃)₃); IR (cm⁻¹) 3330, 1722, 1641, 1137, 1057; MS (*m/z*) [M + H]⁺ 703, [M + Na]⁺ 725, [M + H - CH₂CONHNH₂]⁺ 629.

Synthesis of the Trifluoroacetic Acid Salt of *N*¹,*N*⁷-Bis-guananyl-*N*¹-[*N*-acetylhydrazone(aminoethyl)] Diethylenetriamine. BGTH (Figure 1). Trifluoroacetic acid (150 μL, 1.95 mmol) was added dropwise to a solution of compound 6 (9 mg, 13 μmol) in dichloromethane (1 mL). The reaction mixture was left to stir for 3 h at room temperature upon which the excess trifluoroacetic acid was removed in vacuo. The residue was washed three times with dichloromethane and three times with hexane before evacuating, yielding the product as a clear gel (8 mg, 100%). ¹H NMR (300 MHz, D₂O, CD₃CO₂D) δ 3.97 (s, 2H, CH₂CO), 3.48 (m, 8H, CH₂), 3.30 (t, J_{6,3}, 4H, CH₂); ¹³C NMR (75 MHz, D₂O, CD₃CO₂D) δ 165.13, 163.07 (CO), 156.83 (CN), 51.07, 49.59, 46.38, 45.08, 38.46 (CH₂); MS (*m/z*) [M + H]⁺ 303, [M + 2H]²⁺ 152.

General Procedure for Preparation of Acylhydrazone-Conjugated Cationic Lipids: BGBH-cholest-4-enone as Example (Figures 2 and 3). To a solution of BGBH (48 mg, 80 μmol) in methanol (3 mL) was added 4-cholesten-3-one (31 mg, 81 μmol). Acetic acid (93 μL, 1.64 mmol) was added dropwise, and the solution was left to stir for 24 h. The solvent was removed under vacuum, and the residue was washed four times with hexane before evacuation. The product was revealed as a golden powder on scratching and could be lyophilized to yield a white solid.

Hydrazone from BGBH and 5α-cholestan-3-one, BGBH-cholestanone (Figure 2): ¹H NMR (300 MHz, CD₃OD) δ 3.50, 3.45 (m, 2H, CH₂CO), 3.34 (m, 4H, CH₂NH), 2.99, 2.87 (m, 4H, CH₂N), 2.78–0.80 (m, 43H, steroid portion), 0.72 (s, 3H, 18-CH₃); ¹³C NMR (75 MHz, CD₃OD) δ 173.60, 170.68, 169.05, 166.30 (CO), 157.49 (CN), 56.50, 56.29, 54.33, 53.75 42.38 (CH₂ polyamino portion), 55.62, 55.36, 53.55, 39.92, 39.78, 39.58, 35.96, 35.72, 35.35, 31.92, 31.60, 28.15, 27.92, 27.74, 23.83, 23.54, 21.79, 21.54, 20.92, 17.80, 11.11, 10.48, 10.30 (steroid portion); UV (λ_{max}/nm, 20 mM Hepes) 235 (CN); MS (*m/z*) [M + H]⁺ 629, [M + 2H]²⁺ 315, [BGBH + H]⁺ 260, [cholestanone + H]⁺ 386; HRMS (C₃₅H₆₆ON₉).

Hydrazone from BGBH and cholest-4-en-3-one, BGBH-cholest-4-enone (Figure 2): ¹H NMR (300 MHz, CD₃OD) δ 7.20 (br s, 1H, NH), 6.32, 6.27, 5.94, 5.81 (s, 1H, 4-H), 5.72 (s, 3% residual 4-H of cholestenone), 3.55, 3.49, 3.46 (s, 2H, CH₂CO), 3.26 (m, 4H, CH₂), 2.90 (m, 4H, CH₂), 2.79–1.72 (m, 7H, steroid portion), 1.70–0.80 (m, 33H, steroid portion), 0.72 (s, 3H, 18-CH₃); ¹³C NMR (75 MHz, CD₃OD) δ 170.08, 168.94 (5-C), 162.06, 160.24, 158.14 (CO), 157.51 (CN), 119.52, 114.90 (4-C), 56.18, 56.03, 53.82, 42.17, 37.66 (CH₂ polyamino portion), 55.59, 55.45, 53.55, 39.60, 39.27, 35.92, 35.68, 34.62, 32.10, 27.87, 27.74, 23.81, 23.52, 21.77, 21.52, 21.02, 17.76, 16.67, 10.98 (steroid portion); UV (λ_{max}/nm, 20 mM Hepes) 272 (CN); MS (*m/z*) [M + H]⁺ 627, [M + 2H]²⁺ 314, [cholestenone + H]⁺ 387; HRMS (C₃₅H₆₄ON₉).

Hydrazone from BGTH and 5α-cholestan-3-one, BGTH-cholestanone (Figure 3): ¹H NMR (300 MHz, CD₃OD) δ 4.31, 4.07, 4.04 (s, 2H, CH₂CO), 3.36 (m, 4H, CH₂), 3.25 (m, 2H, CH₂), 2.90 (m, 2H, CH₂), 2.79 (m, 4H, CH₂), 2.65–0.82 (m, 43H,

steroid portion), 0.73 (s, 3H, 18-CH₃); ¹³C NMR (75 MHz, CD₃OD) δ 165.79 (CO), 155.89 (CN), 50.45, 48.79, 44.06, 38.41 (CH₂ polyamino portion), 55.01, 54.79, 52.62, 40.87, 37.77, 37.09, 34.43, 34.19, 33.85, 30.10, 27.11, 26.40, 26.23, 22.32, 22.02, 20.26, 20.02, 19.41, 16.28, 9.58, 9.14, 8.96 (steroid portion); UV (λ_{max}/nm, 20 mM Hepes) 233 (CN); MS (*m/z*) MH⁺ 672, MNa⁺ 694; HRMS (C₃₇H₇₁ON₁₀).

Hydrazone from BGTH and Cholest-4-en-3-one, BGTH-cholest-4-enone (Figure 3): ¹H NMR (300 MHz, CD₃OD) δ 7.12 (br s, 1H, NH), 6.32, 6.27, 5.92, 5.83 (s, 1H, 4-H), 5.72 (s, 8% residual 4-H of cholestenone), 4.32, 4.07 (m, 2H, CH₂CO), 3.36 (m, 4H, CH₂), 3.25 (m, 2H, CH₂), 2.91 (m, 2H, CH₂), 2.79 (m, 4H, CH₂), 2.67–1.75 (m, 6H, steroid portion), 1.70–0.79 (m, 34H, steroid portion), 0.72 (s, 3H, 18-CH₃); ¹³C NMR (75 MHz, (CD₃)₂SO) δ 176.39, 172.69 (5-C), 159.38, 158.97, 158.56, 158.15 (CO), 157.38 (CN), 119.65, 115.68 (4-C), 52.79, 52.57, 52.06, 49.05, 37.66 (CH₂ polyamino portion), 56.00, 53.63, 36.06, 35.60, 31.13, 27.83, 24.25, 23.62, 23.11, 22.85, 21.62, 21.31, 18.96, 12.22 (steroid portion); UV (λ_{max}/nm, 20 mM Hepes) 272 (CN); MS (*m/z*) [M + H]⁺ 670, [M + Na]⁺ 692; HRMS (C₃₇H₆₉ON₁₀).

Hydrolysis Kinetics in Vitro. Hydrolysis experiments were conducted on a Bruker Vector 22 FT-IR spectrophotometer. Experiments were temperature-regulated (25 °C) by an electrical thermosystem and controlled by a temperature sensor immersed within a reference cell containing appropriate buffer. Two buffers were prepared: a sodium acetate/acetic acid buffer at pH 4.8 and a Hepes (20 mM) buffer at pH 7.2. Vectors (~0.3 mg) were dissolved in 3 mL of the appropriate buffer and briefly whirl-mixed until homogeneity was attained, and the solution was placed directly into a quartz cuvette ready for absorbance measurements. Two reference cells, each containing buffer at one of the two pH values, were included in the experiment to observe simultaneously the two sample cells at each of the two pH values. A full wavelength scan of each sample was then made in order to confirm the λ_{max} to be observed during the time-programmed experiment. The absorbances by both sample cells were subsequently taken every 30 min at the defined λ_{max} over a period of 24 h. To ensure that the λ_{max} was followed correctly during the period of the experiment, a range of wavelengths both above and below the λ_{max} were contemporaneously observed and a plot of the reconstituted absorbance curve, viewed as a function of time, was calculated after the experiment. Half-lives were calculated from the best-fit line accorded to the λ_{max} absorbance versus time plot points.

Preparation of Cationic Lipid Formulations. For use as an aqueous solution without liposomal formulation, the reagents were dissolved in water at neutral pH. All reagents were found to be soluble in water, a property likely related to the hydrophilicity of the guanidinium headgroups.

For preparation of liposomes, a mixture of cationic lipid and DOPE (molar ratio 3:2) in chloroform was prepared, and the solvent was evaporated under vacuum. The film of cationic lipid and DOPE was then resuspended in a 20 mM Hepes buffer solution (pH 7.4) to give final total lipid concentrations of either 5 mg/mL for in vitro studies or 5 or 10 mg/mL for in vivo transfections. The mixture was subsequently sonicated (Branson Sonifier 450) for 20 min to form liposomes and filtered through a 0.22 μm filter (Millex GS, Millipore). Liposomes were stored at 4 °C prior to use.

Plasmids. The reporter plasmid pCMV-Luc (kindly provided by B. Demeneix, Museum National d'Histoire Naturelle, Paris, France) used for in vitro transfection has been previously described.^{6,39} Plasmid pCIK-CAT, which was used for the in vivo studies, was obtained from D. Gill (Oxford, U.K.). Briefly, pCIK-CAT was constructed by subcloning the *Escherichia coli* chloramphenicol acetyltransferase (CAT) gene (equipped with a Kozak translation sequence) into a pCI backbone (Promega). The cytosolic luciferase expression plasmid pT7-Luc, where the firefly luciferase reporter gene is under the transcriptional control of the bacteriophage T7 RNA polymerase promoter, was kindly provided by Leaf Huang (Pittsburgh, PA) via P. Midoux (Orléans, France). All plasmids

were amplified in *E. coli* and purified using standard techniques (QIAGEN EndoFree Plasmid Mega Kit).

Preparation of Lipoplexes. Preparation of lipoplexes for in vitro transfection experiments has been described previously.^{38,39} Briefly, plasmid DNA (5 μg) and the desired amount of lipid were each diluted into 250 μL of DMEM without fetal calf serum (FCS) and vortex-mixed. The two solutions were then combined, and the resulting solution was allowed to incubate for 30 min at room temperature. To investigate the effect of serum on transfection efficiency, lipoplexes at a charge ratio of 0.7, 2.0, or 3.9 were first prepared in a total volume of 100 μL of FCS-free DMEM and then an amount of 400 μL of DMEM supplemented with 10% FCS was added to the transfection medium just prior to incubation with the cells.

Preparation of colloiddally stable lipoplexes for in vivo gene transfection into the mouse airways has also been described previously.⁶ Schematically, stable BGBH-cholest-4-enone/DOPE/DNA lipoplexes were obtained in hypotonic medium by adding the steric stabilizer Chol-PEG (kindly provided by C. Masson, Paris, France) to BGBH-cholest-4-enone/DOPE liposomes (in 20 mM Hepes buffer, pH 7.2) immediately prior to mixing with pCIK-CAT DNA in water. Chol-PEG consists of a PEG chain of approximately 100 oxyethylene units linked to a cholesterol anchor.⁶

To determine the theoretical mean charge ratio of the lipoplexes obtained, we took into account that 1 μg of DNA is 3 nmol of negative charges and assumed that only two (the two guanidinium functions in BGBH-cholestanone and BGBH-cholest-4-enone vectors) or three (the two guanidiniums plus the additional secondary amine in BGTH-cholestanone and BGTH-cholest-4-enone vectors) groups were protonated at the neutral pH of lipoplex formation, the central tertiary amino group remaining as a free amine.

Size Determination of Lipid Assemblies and Lipoplexes. Dynamic light scattering analysis was conducted on a Malvern 4700 apparatus at a detection angle of 90°. Size distribution was determined for the BGBH-cholest-4-enone vector formulated alone in aqueous solution as well as for BGBH-cholest-4-enone/DOPE (3/2 molar ratio) liposomes, both being prepared at a concentration of 180 μM of positive charges (90 μM of cationic lipid) in a 20 mM Hepes buffer solution (pH 7.2). Lipoplex samples, characterized by a positive charge ratio of 6, were prepared at a DNA concentration of 10 $\mu\text{g}/\text{mL}$. BGTC-based formulations were prepared and analyzed in an identical manner. Mean particle diameters were determined by multimodal fit analysis.

Cells and Culture Conditions. The in vitro transfection activity of the vectors was evaluated in transient transfection experiments with a variety of mammalian cell lines. The following cell lines were used: HeLa cells that are derived from a human epithelioid cervical carcinoma; COS-7 simian virus-40 transformed monkey kidney cells; HEK 293 adenovirus-transformed human embryo kidney cells; A549 cells derived from a human lung carcinoma; the MITC cell line (a gift from A. Wakkach, Paris, France), which is a human thymic myoid cell line established by immortalizing stromal cells from human thymus.⁴⁹

A T7 RNA polymerase cytoplasmic transcription assay was used to monitor transcribed plasmid in the cytoplasm after lipofection.^{46,50} Here, cytoplasmic luciferase gene expression was evaluated following transfection of the pT7-Luc plasmid (see above) into HEK293-T7 cells. The HEK293-T7 cell line (a gift from Leaf Huang, Pittsburgh, PA, via P. Midoux, Orleans, France) is a 293-cell line producing endogenous T7 RNA polymerase, which was established by cotransfecting 293 cells with pCMV/T7-T7pol and pBK-CMV(neo^r) phagemid with further selection by G418.^{47,51}

All cells were grown in Dulbecco's modified Eagle's medium (DMEM) supplemented with 10% fetal calf serum (FCS), penicillin at 100 units/mL, and streptomycin at 100 $\mu\text{g}/\text{mL}$. Cells were routinely maintained on plastic tissue culture dishes at 37 °C in a humidified 5% CO₂/95% air atmosphere.

In Vitro Transfection, Luciferase Assay, and Determination of Cytotoxicity. In vitro transfection experiments

were performed and luciferase activity was determined as previously described.^{4,38,39} In the cytoplasmic transcription experiments, luciferase expression was analyzed following transfection of HEK293-T7 cells with lipoplexes formed by mixing BGBH-cholest-4-enone (or control BGTC) with either pT7-Luc (cytoplasmic expression) or pCMV-Luc (nuclear expression) plasmid DNA. Here, the cells were harvested and luciferase activity was determined at various post-transfection time points. Data for luciferase activity were expressed as relative light units (RLU) per milligram of cell protein, the protein concentration being determined by the Bio-Rad assay. Cytotoxicity of the lipid formulations was quantified using the total amount of cell protein in the cell lysate (per well) as an index of the cell number. Cytotoxicity data are expressed as concentration of extractable cell protein in the cell lysate (of fixed volume).

Gene Delivery to Mouse Airways and CAT Expression in Vivo. Female BALB/c mice (~30 g body weight) were purchased from Charles River (Saint-Aubin-Les-Elbeuf, France). Intranasal administration of the lipoplexes was conducted as previously described.^{6,39} Schematically, the mice were briefly anesthetized with halothane (Belamont, Paris, France) and instilled intranasally with 50 μL of Chol-PEG-stabilized BGBH-cholest-4-enone/DOPE/pCIK-CAT lipoplexes characterized by a mean positive charge ratio of 3.2 and a Chol-PEG/DNA (w/w) ratio of 2. Each animal received three doses (about 4 h apart), a total amount of 100 μg of pCIK-CAT being administered. At 48 h after instillation, the animals were killed by an ip overdose of pentobarbital and the lungs and trachea were removed for analysis. CAT expression in vivo was evaluated as previously described.^{6,39} In brief, tissue pieces were placed in TEN buffer (40 mM Tris-HCl, 1 mM EDTA, 150 mM NaCl, pH 7.8) and disrupted on ice for about 30 s using an Ultra-Turrax T25 homogenizer (Fisher Bioblock Scientific, Strasbourg, France). Cells were lysed by three freeze-thaw cycles, and the clear supernatant was obtained by centrifugation. CAT concentration was determined using a CAT ELISA assay performed according to the manufacturer's instructions (Boehringer Mannheim). CAT levels were expressed as nanogram of CAT protein per 100 mg of total protein, the protein concentration being determined using the Bio-Rad assay.

Statistical Analysis. Student's *t*-test was used to compare the levels of CAT expression in the lung homogenates obtained with Chol-PEG-stabilized BGBH-cholest-4-enone/DOPE lipoplexes with those obtained in control mice receiving an identical dose of "naked" (uncomplexed) pCIK-CAT plasmid. A *p* value less than 0.05 was considered statistically significant.

Acknowledgment. This work was supported by grants from Vaincre la Mucoviscidose, Association Française contre les Myopathies, and the Marie Curie Individual Fellowship program.

Supporting Information Available: Elemental analyses and high-resolution mass spectrometry data. This material is available free of charge via the Internet at <http://pubs.acs.org>.

References

- Felgner, J. H.; Kumar, R.; Sridhar, C. N.; Wheeler, C. J.; Tsai, Y. J.; Border, R.; Ramsey, P.; Martin, M.; Felgner, P. L. Enhanced gene delivery and mechanism studies with a novel series of cationic lipid formulations. *J. Biol. Chem.* **1994**, *269*, 2550–2561.
- Remy, J.-S.; Sirlin, C.; Vierling, P.; Behr, J.-P. Gene Transfer with a Series of Lipophilic DNA-Binding Molecules. *Bioconjugate Chem.* **1994**, *5*, 647–654.
- Fichert, T.; Regelin, A.; Massing, U. Synthesis and transfection properties of novel non-toxic monocationic lipids. Variation of lipid anchor, spacer and head group structure. *Bioorg. Med. Chem. Lett.* **2000**, *10*, 787–791.
- Vigneron, J. P.; Oudrhiri, N.; Fauquet, M.; Vergely, L.; Bradley, J. C.; Basseville, M.; Lehn, P.; Lehn, J. M. Guanidinium-cholesterol cationic lipids: Efficient vectors for the transfection of eukaryotic cells. *Proc. Natl. Acad. Sci. U.S.A.* **1996**, *93*, 9682–9686.

- (5) Oudrhiri, N.; Vigneron, J. P.; Peuchmaur, M.; Leclerc, T.; Lehn, J. M.; Lehn, P. Gene transfer by guanidinium-cholesterol cationic lipids into airway epithelial cells in vitro and in vivo. *Proc. Natl. Acad. Sci. U.S.A.* **1997**, *94*, 1651–1656.
- (6) Pitard, B.; Oudrhiri, N.; Lambert, O.; Vivien, E.; Masson, C.; Wetzler, B.; Hauchecorne, M.; Scherman, D.; Rigaud, J. L.; Vigneron, J. P.; Lehn, J. M.; Lehn, P. Sterically stabilized BGTC-based lipoplexes: structural features and gene transfection into the mouse airways in vivo. *J. Gene Med.* **2001**, *3*, 478–487.
- (7) Hajri, A.; Wack, S.; Lehn, P.; Vigneron, J.-P.; Lehn, J.-M.; Marescaux, J.; Aprahamian, M. Combined suicide gene therapy for pancreatic peritoneal carcinomatosis using BGTC liposomes. *Cancer Gene Ther.* **2004**, *11*, 16–27.
- (8) Tran, P. L.; Vigneron, J. P.; Pericat, D.; Dubois, S.; Cazals, D.; Hervy, M.; DeClerck, Y. A.; Degott, C.; Auclair, C. Gene therapy for hepatocellular carcinoma using non-viral vectors composed of bis guanidinium-tren-cholesterol and plasmids encoding the tissue inhibitors of metalloproteinases TIMP-2 and TIMP-3. *Cancer Gene Ther.* **2003**, *10*, 435–444.
- (9) Gao, X.; Huang, L. Cationic liposome-mediated gene transfer. *Gene Ther.* **1995**, *2*, 710–722.
- (10) Friend, D. S.; Papahadjopoulos, D.; Debs, R. J. Endocytosis and intracellular processing accompanying transfection mediated by cationic liposomes. *Biochim. Biophys. Acta* **1996**, *1278*, 41–50.
- (11) Xu, Y. H.; Szoka, F. C. Mechanism of DNA release from cationic liposome/DNA complexes used in cell transfection. *Biochemistry* **1996**, *35*, 5616–5623.
- (12) Zelphati, O.; Szoka, F. C. Mechanism of oligonucleotide release from cationic liposomes. *Proc. Natl. Acad. Sci. U.S.A.* **1996**, *93*, 11493–11498.
- (13) Zabner, J.; Fasbender, A. J.; Moninger, T.; Poellinger, K. A.; Welsh, M. J. Cellular and Molecular Barriers to Gene-Transfer by a Cationic Lipid. *J. Biol. Chem.* **1995**, *270*, 18997–19007.
- (14) Aissaoui, A.; Oudrhiri, N.; Petit, L.; Hauchecorne, M.; Kan, E.; Sainlos, M.; Julia, S.; Navarro, J.; Vigneron, J. P.; Lehn, J. M.; Lehn, P. Progress in gene delivery by cationic lipids: Guanidinium-cholesterol-based systems as an example. *Curr. Drug Targets* **2002**, *3*, 1–16.
- (15) Guo, X.; Szoka, F. C., Jr. Chemical Approaches to Triggerable Lipid Vesicles for Drug and Gene Delivery. *Acc. Chem. Res.* **2003**, *36*, 335–341.
- (16) Mukherjee, S.; Ghosh, R. N.; Maxfield, F. R. Endocytosis. *Physiol. Rev.* **1997**, *77*, 759–803.
- (17) Boomer, J. A.; Thompson, D. H.; Sullivan, S. M. Formation of Plasmid-Based Transfection Complexes with an Acid-Labile Cationic Lipid: Characterization of in Vitro and in Vivo Gene Transfer. *Pharm. Res.* **2002**, *19*, 1292–1301.
- (18) Zhu, J.; Munn, R. J.; Nantz, M. H. Self-Cleaving Ortho Ester Lipids: A New Class of pH-Vulnerable Amphiphiles. *J. Am. Chem. Soc.* **2000**, *122*, 2645–2646.
- (19) Mueller, B. M.; Wrasildo, W. A.; Reisfeld, R. A. Antibody conjugates with morpholinodoxorubicin and acid-cleavable linkers. *Bioconjugate Chem.* **1990**, *1*, 325–330.
- (20) Kratz, F.; Beyer, U.; Schumacher, P.; Roth, T.; Zahn, H.; Roth, T.; Fiebig, H. H.; Unger, C. Synthesis of new maleimide derivatives of daunorubicin and biological activity of acid labile transferrin conjugates. *Bioorg. Med. Chem. Lett.* **1997**, *7*, 617–622.
- (21) Kaneko, T.; Willner, D.; Monkovic, I.; Knipe, J. O.; Braslawsky, G. R.; Greenfield, R. S.; Vyas, D. M. New hydrazone derivatives of adriamycin and their immunoconjugates. A correlation between acid stability and cytotoxicity. *Bioconjugate Chem.* **1991**, *2*, 133–141.
- (22) Rodrigues, P. C. A.; Beyer, U.; Schumacher, P.; Roth, T.; Fiebig, H. H.; Unger, C.; Messori, L.; Orioli, P.; Paper, D. H.; Mulhaupt, R.; Kratz, F. Acid-sensitive polyethylene glycol conjugates of doxorubicin: Preparation, in vitro efficacy and intracellular distribution. *Bioorg. Med. Chem.* **1999**, *7*, 2517–2524.
- (23) Kratz, F.; Beyer, U.; Schutte, M. T. Drug-polymer conjugates containing acid-cleavable bonds. *Crit. Rev. Ther. Drug Carrier Syst.* **1999**, *16*, 245–288.
- (24) Gerasimov, O. V.; Boomer, J. A.; Qualls, M. M.; Thompson, D. H. Cytosolic drug delivery using pH- and light-sensitive liposomes. *Adv. Drug Delivery Rev.* **1999**, *38*, 317–338.
- (25) Drummond, D. C.; Zignani, M.; Leroux, J. Current status of pH-sensitive liposomes in drug delivery. *Prog. Lipid Res.* **2000**, *39*, 409–460.
- (26) Liang, E.; Hughes, J. Characterization of a pH-sensitive surfactant, dodecyl-2-(1'-imidazolyl) propionate (DIP), and preliminary studies in liposome mediated gene transfer. *Biochim. Biophys. Acta* **1998**, *1369*, 39–50.
- (27) Boomer, J. A.; Inerowicz, H. D.; Zhang, Z.-Y.; Bergstrand, N.; Edwards, K.; Kim, J.-M.; Thompson, D. H. Acid-Triggered Release from Sterically Stabilized Fusogenic Liposomes via a Hydrolytic DePEGylation Strategy. *Langmuir* **2003**, *19*, 6408–6415.
- (28) Kumar, V. V.; Pichon, C.; Refregiers, M.; Guerin, B.; Midoux, P.; Chaudhuri, A. Single histidine residue in head-group region is sufficient to impart remarkable gene transfection properties to cationic lipids: evidence for histidine-mediated membrane fusion at acidic pH. *Gene Ther.* **2003**, *10*, 1206–1215.
- (29) Budker, V.; Gurevich, V.; Hagstrom, J. E.; Bortzov, F.; Wolff, J. A. pH-sensitive, cationic liposomes: a new synthetic virus-like vector. *Nat. Biotechnol.* **1996**, *14*, 760–764.
- (30) Bell, P. C.; Bergsma, M.; Dolbnya, I. P.; Bras, W.; Stuart, M. C. A.; Rowan, A. E.; Feiters, M. C.; Engberts, J. B. F. N. Transfection Mediated by Gemini Surfactants: Engineered Escape from the Endosomal Compartment. *J. Am. Chem. Soc.* **2003**, *125*, 1551–1558.
- (31) Frederic, M.; Scherman, D.; Byk, G. Introduction of cyclic guanidines into cationic lipids for non-viral gene delivery. *Tetrahedron Lett.* **2000**, *41*, 675–679.
- (32) Frey, B. M.; Benassi, R.; Taddei, F. Theoretical-Study of Conformational-Changes in Simple Hydrazones. *J. Chem. Soc., Perkin Trans. 2* **1985**, 1629–1632.
- (33) Palla, G.; Predieri, G.; Domiano, P.; Vignali, C.; Turner, W. Conformational Behavior and E/Z Isomerization of N-Acyl and N-Aroylhydrazones. *Tetrahedron* **1986**, *42*, 3649–3654.
- (34) Gasparro, F. P.; Kolodny, N. H. NMR Determination of the Rotational Barrier in N,N-dimethylacetamide. *J. Chem. Educ.* **1977**, *54*, 258–261.
- (35) Wheeler, O. H.; Rosado-Lojo, O. Kinetics of formation and hydrolysis of steroid Girard-T hydrazones. *Tetrahedron* **1962**, *18*, 477–482.
- (36) Greene, T. W.; Wuts, P. G. *Protective Groups in Organic Synthesis*, 2nd ed.; John Wiley & Sons: New York, 1991.
- (37) Dietrich, B.; Hosseini, M. W.; Lehn, J. M.; Sessions, R. B. Synthesis and protonation features of 24-, 27- and 32-membered macrocyclic polyamines. *Helv. Chim. Acta* **1983**, *66*, 1262–1278.
- (38) Patel, M.; Vivien, E.; Hauchecorne, M.; Oudrhiri, N.; Ramasawmy, R.; Vigneron, J. P.; Lehn, P.; Lehn, J. M. Efficient gene transfection by bisguanilylated diacetylene lipid formulations. *Biochem. Biophys. Res. Commun.* **2001**, *281*, 536–543.
- (39) Belmont, P.; Aissaoui, A.; Hauchecorne, M.; Oudrhiri, N.; Petit, L.; Vigneron, J.-P.; Lehn, J.-M.; Lehn, P. Aminoglycoside-derived cationic lipids as efficient vectors for gene transfection in vitro and in vivo. *J. Gene Med.* **2002**, *4*, 517–526.
- (40) Marshall, J.; Nietupski, J. B.; Lee, E. R.; Siegel, C. S.; Rafter, P. W.; Rudginsky, S. A.; Chang, C. D.; Eastman, S. J.; Harris, D. J.; Scheule, R. K.; Cheng, S. H. Cationic lipid structure and formulation considerations for optimal gene transfection of the lung. *J. Drug Targeting* **2000**, *7*, 453–469.
- (41) Gao, X.; Huang, L. A novel cationic liposome reagent for efficient transfection of mammalian cells. *Biochem. Biophys. Res. Commun.* **1991**, *179*, 280–285.
- (42) Zhou, X.; Huang, L. DNA transfection mediated by cationic liposomes containing lipopolylysine: characterization and mechanism of action. *Biochim. Biophys. Acta* **1994**, *1189*, 195–203.
- (43) Pitard, B.; Oudrhiri, N.; Vigneron, J. P.; Hauchecorne, M.; Aguerre, O.; Toury, R.; Airiau, M.; Ramasawmy, R.; Scherman, D.; Crouzet, J.; Lehn, J. M.; Lehn, P. Structural characteristics of supramolecular assemblies formed by guanidinium-cholesterol reagents for gene transfection. *Proc. Natl. Acad. Sci. U.S.A.* **1999**, *96*, 2621–2626.
- (44) Hoekstra, D.; Scherphof, G. Effect of fetal calf serum and serum protein fractions on the uptake of liposomal phosphatidylcholine by rat hepatocytes in primary monolayer culture. *Biochim. Biophys. Acta* **1979**, *551*, 109–121.
- (45) Yang, J. P.; Huang, L. Overcoming the inhibitory effect of serum on lipofection by increasing the charge ratio of cationic liposome to DNA. *Gene Ther.* **1997**, *4*, 950–960.
- (46) Gao, X.; Jaffurs, D.; Robbins, P. D.; Huang, L. A sustained, cytoplasmic transgene expression system delivered by cationic liposomes. *Biochem. Biophys. Res. Commun.* **1994**, *200*, 1201–1206.
- (47) Brisson, M.; Tseng, W. C.; Almonte, C.; Watkins, S.; Huang, L. Subcellular trafficking of the cytoplasmic expression system. *Hum. Gene Ther.* **1999**, *10*, 2601–2613.
- (48) Fujiwara, T.; Hasegawa, S.; Hirashima, N.; Nakanishi, M.; Ohwada, T. Gene transfection activities of amphiphilic steroid-polyamine conjugates. *Biochim. Biophys. Acta* **2000**, *1468*, 396–402.
- (49) Wakkach, A.; Poeta, S.; Chastre, E.; Gespach, C.; Lecerf, F.; De La Porte, S.; Tzartos, S.; Coulombe, A.; Berrich-Aknin, S. Establishment of a human thymic myoid cell line. Phenotypic and functional characteristics. *Am. J. Pathol.* **1999**, *155*, 1229–1240.
- (50) Gao, X.; Huang, L. Cytoplasmic expression of a reporter gene by co-delivery of T7 RNA polymerase and T7 promoter sequence with cationic liposomes. *Nucleic Acids Res.* **1993**, *21*, 2867–2872.
- (51) Li, S.; Brisson, M.; He, Y.; Huang, L. Delivery of a PCR amplified DNA fragment into cells: a model for using synthetic genes for gene therapy. *Gene Ther.* **1997**, *4*, 449–454.